Kurdistan Journal of Applied Research (KJAR)
Print-ISSN: 2411-7684 | Electronic-ISSN: 2411-7706

Original Article

Novel Fluorinated Pyrazoline Based Ethers: Synthesis, Characterization and Antimicrobial Evaluation

Zheena Jabar Mustafa [a *], **Twana Mohsin Salih** [a], **Farouq Emam Hawaiz** [b]

[a] Department of Pharmacognosy and Pharmaceutical Chemistry, College of Pharmacy, University of Sulaimani, Sulaymaniyah, Iraq.
[b] Department of Chemistry, College of Education, University of Salahaddin, Hawler, Iraq.

Submitted: 21 August 2025
Revised: 4 October 2025
Accepted: 2 November 2025

*** Corresponding Author**:
zheena.mustafa@univsul.edu.iq

Keywords: Benzyloxy, Chalcone, Claisen-Schmidt condensation, Pyrazoline; Gram-positive and gram-negative bacteria, One-pot synthesis.

How to cite this paper: Z. J. Mustafa, T. M. Salih, F. E. Hawaiz,"Novel Fluorinated Pyrazoline Based Ethers: Synthesis, Characterization and Antimicrobial Evaluation", KJAR, vol. 10, no. 2, pp: 284-306, Dec 2025, doi: 10.24017/science.2025.2.18

Abstract: In response to the growing global threat of antimicrobial resistance, this work seeks to synthesize and analyze chalcone-derived pyrazoline derivatives and assess their antibacterial efficacy against the Staphylococcus aureus and Escherichia coli). A series of pyrazoline compounds were synthesized using both classical step-wise and one-pot synthetic strategies, involving Claisen–Schmidt condensation of 4-(4-fluorobenzyl) oxy acetophenone with various substituted benzaldehydes that subsequently undergo cyclization with phenyl hydrazine. The chemical structures of the produced chalcones and their corresponding pyrazolines were characterized using FTIR, ^{1}H-NMR, and ^{13}C-NMR spectroscopy. Physicochemical characterization revealed the products were obtained in high yields and were sufficiently stable for isolation, with improved yields observed via the one-pot method. Antibacterial activity was assessed using the disk diffusion technique at multiple concentrations (200–800 ppm). The results demonstrated that pyrazoline derivatives exhibited significantly higher inhibition zones, particularly against S. aureus, compared to their chalcone precursors. Compounds 5a, 5c, and 5f had the most significant antibacterial efficacy, whereas chalcones showed minimal to no action against E. coli. The findings confirm the superior bioactivity of the pyrazoline ring system and suggest the crucial impact of electron- giving and electron-removing substituents on antibacterial potential. This research underscores one-pot synthesis as operationally simple and reducing waste generation by eliminating the need for intermediate isolation, thereby offering a more efficient and practical route, time-saving method for producing structurally varied, physiologically active pyrazolines, presenting attractive possibilities for the development of novel antibacterial medicines.

1. Introduction

Infections and the escalating resistance of microorganisms to conventional antibacterial therapies are major global health concerns that contribute to a wide range of diseases affecting humanity [1]. It is estimated that about 250 million bacterial infection cases occur annually, leading to around $1.6 billion in economic losses each year [2]. Consequently, the rates of hospitalization and death increase substantially. Antimicrobial resistance is an ongoing issue of concern in the United States and worldwide [3]. Antibacterial resistance is responsible for more than 700,000 deaths globally each year [4]. Projections indicate Fatalities may escalate to 10 million per year by 2050 if effective treatments are not enacted [5]. Approximately 2.8 million individuals are afflicted with drug-resistant pathogens, resulting in over 35,000 fatalities annually in the United States alone [2, 3]. In the absence of prompt and concerted measures we are progressing toward a period where common place diseases or small injuries might become lethal, Thus, it is vital to investigate the advancement of novel and efficacious antibiotics [6].

These developments seek to mitigate the effects of illnesses that existing antibiotics can no longer effectively treat [7]. Therefore, it is strongly advised to prioritize the design, development, and synthesis of new compounds that exhibit superior antibacterial activity and diminished hazards [8].

The Claisen–Schmidt condensation method substitutes acetophenones and benzaldehydes to produce chalcones. These chemicals, characterized by the overall formula Ar–CO–CH=CH–Ar (1,3-diphenyl-2-propen-1-one), are classified as part of the flavonoid family [9]. The molecular formula of chalcone, $C_{15}H_{12}O$, exhibits two stereochemical configurations: cis and trans, with the trans configuration being (-1,3-diphenyl-2-propene-1-one) [10]. The trans isomer is more stable and dominant, but the cis isomer is unstable due to steric interactions between the carbonyl group and the A-ring [11]. They occur naturally and can also be synthesized, functioning as significant intermediates in advanced chemistry. Their scientific importance is due to the existence of many replaceable hydrogens, facilitating the synthesis of diverse derivatives [12]. Consequently, they are considered the foundation for the synthesis of several chemicals, including pyrazoline, thiazine, and pyrimidine [13]. Diverse methods for chalcone synthesis include Claisen-Schmidt, Suzuki, Wittig, and Friedel-Crafts acylation [14]. The Claisen-Schmidt condensation, sometimes referred to as Aldol condensation, is a widely utilized process characterized by its simplicity and high yield ranging from 60% to 90% [15]. Chalcones are defined as α, β-unsaturated carbonyl compounds, with two electrophilic sites resulting from the delocalization of electron density inside the C=C–C=O structure [16]. The electrical structure enables chalcones to easily participate in nucleophilic addition reactions, which can occur by direct assault on the carbonyl carbon (1,2-addition) or at the β-carbon of the enone system (1,4-conjugate or Michael addition) [17]. Such reactivity underpins their role as key precursors in the synthesis of diverse bioactive heterocyclic frameworks. A notable example is the formation of 2-pyrazolines, which are typically obtained through cyclization reactions involving chalcones and hydrazine derivatives [18]. These transformations not only highlight the synthetic versatility of chalcones but also emphasize their importance in medicinal chemistry for generating compounds with potential pharmacological applications [19].

Pyrazoline and its derivatives have demonstrated considerable biological activity [20]. The molecule is regarded as a neutrophil agent, thereby playing a significant role in different pharmacological actions, including anti-inflammatory and anti-microbial effect [21]. Dihydropyrazole, also referred to as Pyrazolines, are five-membered heterocyclic compounds that exhibit considerable stability owing to the presence of two adjacent nitrogen atoms within the ring and the endocyclic double bond [22]. The location of this double bond distinguishes the three potential isomeric forms: 1-pyrazoline, 2-pyrazoline, and 3-pyrazoline, each displaying unique structural and electronic properties that affect their chemical reactivity and biological activity [23].

Chalcones and their pyrazoline derivatives are important compounds in medicinal chemistry due to their potential biological effects, including antioxidation [24], anticancer [25], antibacterial [26, 27], antidiabetic [28] , antiulcer [29], antiviral [30], anti-HIV, anti-protozoal [31], anti-gout [22], antihypertensive [32], anti-obesity [33], anti-histaminic [34], hypnotic [35], anticonvulsant [36], antitubercular [37], antimalarial [38], and anti-angiogenic properties [39].

Research indicates that the α, β-unsaturated ketone is a contributing factor to antibacterial action [40]. For chalcones, antibacterial activity depends on the scaffold and on factors such as the tested bacterial strain and its characteristics, molecular size, lipophilicity, and the number and position of ring substituents [41]. The modification of functional groups in chalcone derivatives—for instance, substituting a hydroxyl group with a carboxyl moiety on either the A or B aromatic ring—can significantly improve their solubility as well as modulate their biological properties [42]. In chalcone-derived pyrazolines, the coexistence of conjugated phenyl rings and C=N functionalities promotes extensive electron delocalization and resonance stabilization [43]. This electronic distribution not merely augments the structural stability of the molecules but also serves a crucial function in ascertaining their biological efficiency and pharmacological potential [44]. Cyclization predominantly enhances antibacterial properties; nevertheless, in certain instances, it may diminish efficacy due to molecular incompatibility with bacterial characteristics [45]. The introduction of electron-donating groups and electron-withdrawing groups, including phenyl and nitro substituents, into the pyrazoline framework has been documented to influence antibacterial activity in various manners [46]. Furthermore, the location of the double bond

inside the pyrazoline ring system significantly affects the overall biological activity of these molecules, underscoring the importance of structural and electronic factors in their pharmacological performance [47].

The one-pot synthesis method offers a direct pathway wherein α, β-unsaturated aldehydes and acetophenones react with hydrazine derivatives to generate the requisite goods in a singular phase [48]. In contrast, the step-wise method is more commonly employed, involving the initial preparation of the corresponding chalcone intermediate. This is then treated to cyclization with hydrazine to get the desired molecules [49].

In 2008, Traven *et al.* [50] presented a one-pot synthesis method for the production of 1,3,5-triaryl-2-pyrazolines. The synthesis entailed a reaction. Aryl aldehydes, acetophenone, and phenyl hydrazine are employed with NaOH as a base, with the reflux length surpassing 40 minutes in ethanol to get a 78% yield [51]. The synthesis of pyrazoline using a two-pot approach is more frequently documented than use of a one-pot technique, the two-pot process being the traditional approach [52]. The process had two primary phases: initially, the synthesis of chalcones, succeeded by cyclization using hydrazine hydrate under regulated reaction conditions [53]. Subsequently, other synthetic methods were documented in which chalcones acted as precursors to pyrazolines, employing various solvents or catalysts in basic, acidic, or neutral environments [54]. The Claisen–Schmidt condensation under alkaline circumstances is the most extensively documented technique for the efficient synthesis of chalcones [55]. In organic chemistry, key considerations include environmental sustainability, safety, economic feasibility, and overall process efficiency. These aspects require considerable consideration, especially when synthesizing fragile and expensive materials and compounds that need multi-step procedure [56]. Recent developments in one-pot synthesis methods for the production of complex physiologically active molecules have emerged as a major emphasis in medical research, especially in organic and combinatorial chemistry [57]. The one-pot approach is a novel technique that integrates several synthetic steps into a single reaction system, facilitating the synthesis of the target compound without the need for isolating intermediate products [58]. This technology has several advantages, such as reduced chemical waste, compliance with ecologically sustainable practices, economic viability, operational ease, and significantly decreased reaction times [59]. However, the one-pot process has several limitations, including the formation of undesirable compounds that increase under varying reaction conditions [60]. On the other hand, while the two-pot synthetic method has the advantage of enhanced product purity, its drawbacks are prolonged reaction time, elevated temperature, and laborious two-step procedures [61].

Fluorine-containing compounds have garnered significant industrial attention during the past two decades [62]. Effective synthetic methods have been established to incorporate fluorine into heterocyclic structures during compound synthesis, aimed at improving their suitability for medicinal applications [63]. Nitrogen-based heterocyclic compounds are extensively investigated for their potential therapeutic applications and for their importance in the discovery of novel biologically active molecules [64]. In fluorinated heterocyclic compounds, the inclusion or replacement of fluorine for a hydrogen atom can modify reaction pathways, rendering them scientifically significant due to their considerable potential in drug creation [65]. The integration of a trifluoromethyl group with a heterocyclic structure has been documented to possess considerable pharmacological significance in fluorine-containing drugs [66]. Replacing hydrogen with fluorine atoms modifies key physicochemical properties—including electronegativity, inductive effects, lipid solubility, and binding affinity—thereby enhancing the bioactivity of the compound [67]. Fluorine-containing compounds frequently demonstrate enhanced biological activity and decreased toxicity compared to their hydrogen counterparts [68]. The existence of reduced fluorine atom concentration does not significantly influence pharmacological inhibition through cellular receptors [69]. Consequently, clusters of fluorine atoms have been used in several biological systems instead of hydrogen atoms [70]. Fluorine atoms, characterized by their stable C-F bonds, small size, and strong electronegativity, have been employed as halogens in pharmacodynamics and chemotherapeutic medicines [71]. Fluorine-substituted compounds exhibit significant applications in both medical and non-medical fields, including dyes, polymers, agrochemicals, analgesics, and antipyretics [72]. This work investigates the synthesis and characterization of new chalcone-derived

pyrazoline compounds by stepwise and one-pot three-component processes, thereafter conducting antimicrobial screening to assess their efficacy against common pathogenic strains.

2. Materials and Methods

The reagents used throughout this study were purchased from Sigma-Aldrich (St. Louis, MO, USA) and Merck (Germany). Melting points of the synthesized compounds were measured using a Stuart automatic melting point apparatus (Barloworld Scientific Ltd., Staffordshire, UK a commonly used technique for characterizing purity and thermal stability) [73]. Solvent removal was performed with a Heidolph rotary evaporator equipped with a digital heating bath (HB digit, Germany) [74]. Infrared (IR) spectra were recorded on a Shimadzu FTIR-8400s spectrophotometer (Japan), with the samples prepared in potassium bromide disks. Reaction progress was tracked by thin-layer chromatography (TLC) using silica gel 60 F254 aluminum plates (Sigma-Aldrich, Canada) and a mobile phase of hexane and ethyl acetate (7:3) [75]. Proton (^{1}H) and carbon (^{13}C) nuclear magnetic resonance (NMR) spectra were obtained on a Bruker UltraShield 400 MHz instrument, with tetramethylsilane as the internal standard and deuterated chloroform ($CDCl_3$) as the solvent [76].

2.1. Methods

2.1.1. Synthesis of Starting Materials: Preparationof4-(4-Fluorobenzyl) oxyacetophenone(1),4-((4-fluorobenzyl) oxy) benzaldehyde (2), 2,3-bis(4-fluorobenzyloxy) benzaldehyde (3)

4-Hydroxyacetophenone, 4-hydroxybenzyldehyde, or 2,3-dihydroxybenzyl aldehyde (0.03 moL) was combined with 4-fluorobenzyl bromide (8.49 g, 0.044 moL) and anhydrous K_2CO_3 (12.42 g, 0.09 moL) in absolute ethanol (60 mL) within a 500 mL round-bottom flask and refluxed for 9, 10, and 12 hours with stirring [77]. After the reaction concluded, it was assessed by TLC and the solution's color change. Thereafter, the surplus solvent was eliminated using rotational evaporation. After the reaction was completed, the fluid was cooled and then poured onto crushed ice, resulting in the instantaneous precipitation of solid products [78]. Solids were obtained using filtering, subsequently rinsed with 100 mL of cold distilled water and cold ethanol, and then dried and purified via recrystallization from ethanol., and then dried and purified through recrystallization from ethanol. This process produced white crystalline forms of benzyloxy acetophenone (1), benzyloxy benzaldehyde (2), and benzyloxy dihydroxy benzaldehyde (3), each acquired in different colors and yields [79].

2.1.2. Synthesis of Chalcone (4a and 4b)

A combination of compound 1 (0.004 moL, 1.00 g) and the corresponding substituted benzaldehyde (0.004 moL) in ethanol (30 mL) was subjected to treatment with ethanolic NaOH (4%, 4 mL) and stirred under reflux at 78 °C for 45 minutes [80]. The resultant precipitate was filtered, rinsed with cold distilled water, dried, and recrystallized using ethanol. Chalcone 4a ($C_{23}H_{19}FO_2$, M = 346.39 g/moL)**:** theoretical yield 1.39 g (0.0040 moL); actual yield 1.04 g (0.0030 moL, 75%). Chalcone 4b ($C_{23}H_{19}FO_2S$, M = 378.46 g/moL): theoretical yield 1.51 g (0.0040 moL); actual yield 1.15 g (0.0030 moL, 76%). Progress was assessed through the formation of a precipitate (TLC), employing n-hexane: ethyl acetate (7:3) as the eluent, and alterations in solution color [81]. The reaction mixture was concentrated to 10 mL, cooled, and the resultant precipitate was collected via filtering, washed with 100 mL of cold distilled water, and recrystallized with ethanol. The products 4a and 4b were synthesized in varying hues and yields [82].

2.1.3. One-pot Synthesis of Pyrazoline. 3-(4-((4-fluorobenzyl) oxy) phenyl) -5-(substituted phenyl) -4,5-dihydro-1H-pyrazole (5a-i)

In the one-pot method, compound 1 (0.004 moL, 1.00 g) and a substituted benzaldehyde (0.004 moL) were solubilized in 30 mL of pure ethanol within a 100 mL round-bottom flask fitted with a reflux condenser. Sodium hydroxide (4% in ethanol, 4 mL; 1.0 equivalents relative to the carbonyl component) was added dropwise with agitation, and the reaction was subjected to reflux at 78 °C for 45 minutes [83]. This facilitated the in situ Claisen–Schmidt condensation to give the chalcone intermediate. Based on 0.004 moL of limiting reagent, the theoretical yields were 1.39 g (0.0040 moL) for compound 4a and

1.51 g (0.0040 moL) for compound 4b. The actual isolated chalcones were obtained in 1.04 g (0.0030 moL, 75%) for 4a and 1.15 g (0.0030 moL, 76%) for 4b. Without isolating the intermediate, phenylhydrazine (0.006 moL) was included directly into the reaction mixture, which was subjected to reflux at 78 °C for 9 hours. The progression of the reaction was observed by TLC, employing a solvent system of n-hexane and ethyl acetate in a 7:3 ratio. as eluent, along with visual color changes. After completion, the liquid was concentrated to 10 mL under decreased pressure and subsequently chilled. The precipitated pyrazolines were obtained via filtering, rinsed with cold water, dried, and recrystallized from a methanol/ethanol mixture in a 2:10 ratio. The pyrazolines were synthesized in quantities of 0.83 g (0.0019 moL, 94%) for compound 5h and 0.80 g (0.0019 moL, 94%) for compound 5i, relative to their theoretical yields of 0.88 g (0.0020 moL) and 0.85 g (0.0020 moL), respectively [84].

2.1.4. Two Pot Synthesis of Pyrazolines

In the two-pot method, chalcone derivatives 4a (2.0 mmoL, 0.69 g) or 4b (2.0 mmoL, 0.76 g) were dissolved in 15 mL of absolute ethanol in a 50 mL round-bottom flask fitted with a reflux condenser. Phenylhydrazine (2.0 mmoL, 0.22 g; 1.0 equiv relative to chalcone) and ethanolic NaOH (4%, 0.5 mL; ~0.5 equiv) were then added. The combination was refluxed at 78 °C for a duration of 6 to 8 hours with continuous agitation. The course of the reaction was tracked by TLC (n-hexane: ethyl acetate, 7:3) and by observing visible color changes [85]. Upon completion, the solvent was concentrated under reduced pressure to approximately 10 mL and subsequently chilled to ambient temperature. The precipitated material was obtained using vacuum filtering, rinsed with cold distilled water (3 × 30 mL), dried, and recrystallized from a methanol/ethanol combination (1:1) to get the desired pyrazolines. Compound 5h ($C_{28}H_{24}FNOS$, M = 441.56 g/moL): Theoretical yield 0.88 g (0.0020 moL); actual yield 0.83 g (0.0019 moL, 94%). Compound 5i ($C_{28}H_{25}FN_2O$, M = 424.51 g/moL): theoretical yield 0.85 g (0.0020 moL); actual yield 0.80 g (0.0019 moL, 94%). In some protocols, a slight excess of phenylhydrazine (1.2–1.5 equivalents) is employed to ensure complete cyclization, since hydrazine derivatives can partially decompose under reflux or be hindered by steric effects. In this work, however, stoichiometric amounts (1.0 equivalents) relative to chalcone were sufficient to achieve excellent yields [85]. Figure 1 shows one-pot and stepwise synthetic process for new pyrazoline derivatives featuring benzyloxy moieties.

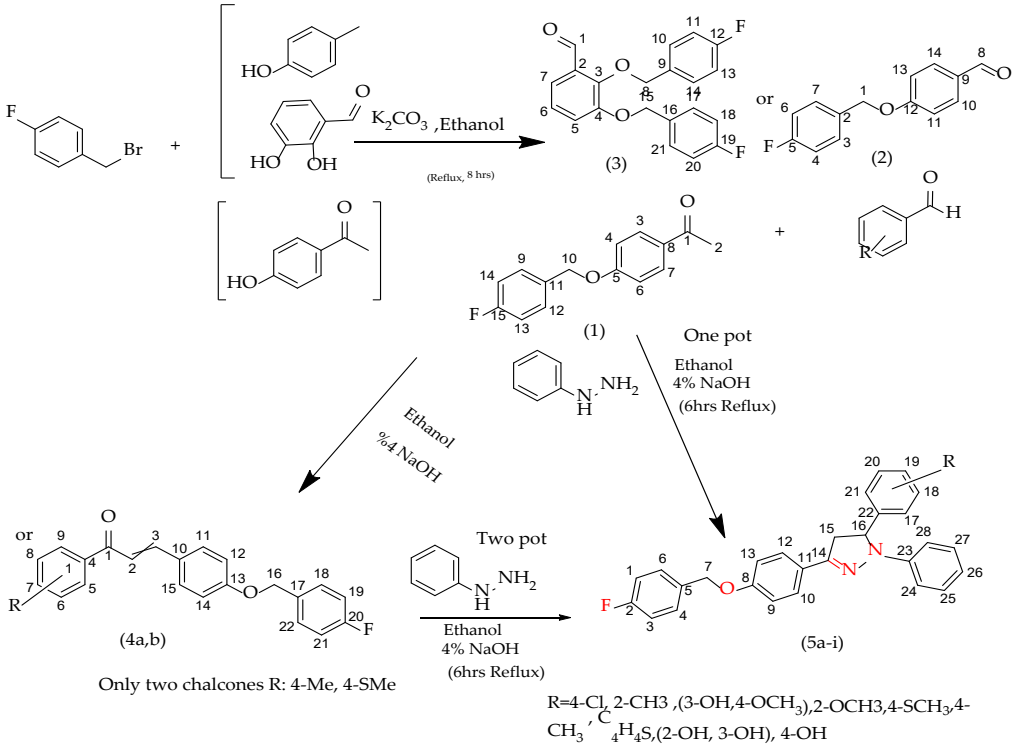

Figure 1: A one-pot and stepwise synthetic process for new pyrazoline derivatives featuring benzyloxy moieties is presented.

2.1.5. Patterns of Antimicrobial Effectiveness of Synthesized Pyrazoline Derivatives Against Gram-positive Bacteria Staphylococcus aureus and Gram-negative Bacteria Escherichia coli

Synthesized chalcone and pyrazine derivatives were tested against *E. coli* ATCC 8739 (Gram-negative) and *S. aureus* ATCC 6538 (Gram-positive) using the disc diffusion technique and were tested based on Clinical and Laboratory Standards Institute guidelines (M02-A13; M07-A10). Fresh cultures were prepared by inoculating a single colony of each strain on blood agar and incubating at 37 ℃ for 24 h. To prepare broth, 2.10 g of Mueller Hinton broth was put in 100 mL of distilled water and warmed to complete dissolution, and then autoclaved at 121 ℃ and 15 minutes to sterilize it. One fresh colony was then inoculated into the broth and incubated at 37 ℃ for 24 h. Following spectrophotometric modification at 600 nm (OD600 = 0.080.10) was a method of standardizing the bacterial suspension to a 0.5 McFarland standard (approximately 1.5 x 108 CFU/mL) and visually cross-checking the suspension assessment against a McFarland standard reference tube [86]. Mueller Hinton agar was prepared by placing 19 g of the dehydrated medium in 500 mL distilled water, heating to complete dissolution, autoclaving at 121 °C at 15 minutes, and then letting the solution cool back to 45-50 ℃. The medium was poured into the sterile Petri dishes to a depth of 4 mm (apx 25 mL/90 mm plate) under a laminar flow hood and left to solidify at room temperature. Preparation of the sterile filter paper disks (6 mm in diameter) was done using autoclave. N, N-dimethylformamide (DMF) was used as the solution for the test solutions at 200, 400, 600, and 800 ppm. On a sterile disc, one pipette of solution/disc was applied (2, 4, 6, and 8 μg/disc) to each concentration. The discs were dried at room temperature in an aseptic condition, after impregnation. All the materials (discs, test tubes, Petri dishes, filters, and micropipette tips) were autoclaved prior to use. To avoid contamination, the DMF solvent was filtered by a 0.22 μm antibacterial filter. Distribution of the standardized bacterial suspension was done in a uniform manner on the surface of the Mueller Hinton agar plates. Inoculated plates with the impregnated discs were put together with a DMF-only disc (negative control) and commercial amoxicillin disc (10 μg/disc, Oxoid, UK) as the positive control (10 μg/disc, positive control). Aerobic incubation of the plates at 37 ℃ was undertaken over a period of 24 h. A Vernier caliper was used to measure millimeter-wise the inhibition zones to the nearest one-tenth.

2.2 Statistical Analysis

Each assay was conducted thrice (n = 3), and the results were presented as mean and standard deviation. In cases where no inhibition zone was observed, the outcome was taken as 0 (no inhibition zone observed) [87], with the millimeters of inhibition shown in tables S1 and S2. To evaluate differences in antibacterial activity among the synthesized compounds at each concentration, a one-way Analysis of Variance (ANOVA) was applied. When the ANOVA results indicated significant differences ($p < 0.05$), Tukey's Honest Significant Difference (HSD) post-hoc test was performed for pairwise comparison of means. All calculations were performed using SPSS software package version 26 (IBM Corp., Armonk, NY, USA).

3. Results

3.1. Characterization Results of Starting Compounds

3.1.1. 4-(4-Fluorobenzyl) oxyacetophenone (1)

$C_{15}H_{13}FO_2$. m.p. (78-80) °C, (90%), color (white), IR (cm^{-1}) str. 3066 (C-H), 2919-2873 (C-H), 1681 (C=O), 1600 (C=C), 1234 (C-O-C), 1010 (C-F), 831 (C-H) ^{1}H-NMR. (ppm): 2.55 (3H, s, CH_3–CO), 5.09 (2H, s, Benzylic –CH_2–O–), 6.96-7.11 (4H, m, AR-$H_{3,4,7,6}$), 7.39-7.96 (4H, m, AR-$H_{9,14,12,13}$). ^{13}C-NMR (ppm), 196: C_1, 163: C_5, 162.49: C_{15}, 161.48: C_{13}, 132.01: C_{11}, 131.98: C_3, 130.73: C_7, 130.67: C_9, 129.56: C_{12}, 129.48: C_8, 115.85: C_{14}, 115.64: C_6, 114.56: C_4, 69.51: C_{10}, 26.51: C_2. Figure 2 illustrates the confirmed structure of 4-(4-fluorobenzyl) oxyacetophenone ($C_{15}H_{13}FO_2$) obtained from spectral characterization.

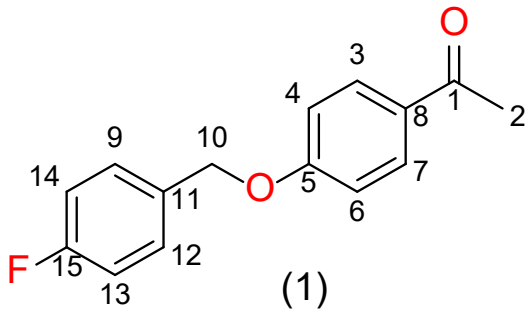

Figure 2: Sructure of 4-(4-Fluorobenzyl) oxyacetophenone (1).

3.1.2. 4-((4-fluorobenzyl) oxy) benzaldehyde (2)

$C_{14}H_{11}FO_2$, m.p. (100-103) °C, (92%), color (white), IR (cm^{-1}) str. 3048 (C-H), 2947 (C-H), 2768-2846 (Aldehyde C–H stretch), 1684 (Aldehyde C=O), 1603 (C=C), 1253 (C-O-C), 998 (C-F), 850 (C-H). ^{1}H-NMR (ppm): 9.89 (1H, s, –CHO), 7.06-7.11 (4H, m, Ar-$H_{13,14,11,10}$), 7.40-7.86 (4H, m, Ar$H_{6,7,4,3}$), 5.11 (2H, s, OCH_2). ^{13}CNMR (ppm): 190.93: C_8, 163.98: C_5, 163.60: C_{12}, 161.52: C_{10}, 132.13: C_{14}, 131.79: C_3, 131.76: C_7, 130.27: C_9, 129.51: C_{13}, 129.60: C_2, 115.17: C_6, 115.69: C_{11}, 115.90: C_4, 69.66: C_1. Figure 3 illustrates the confirmed structure of 4-(4-fluorobenzyl) oxyacetophenone ($C_{14}H_{11}FO_2$) as established from the spectral characterization data.

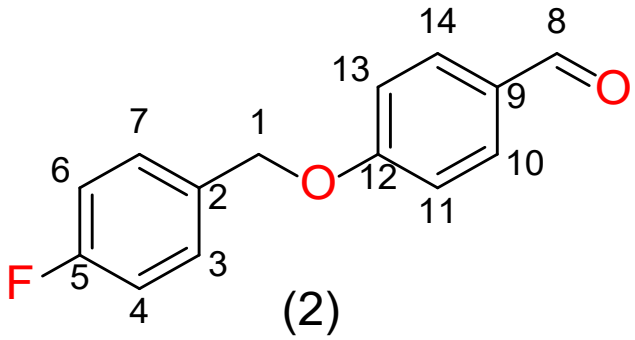

Figure 3: Structure of 4-((4-fluorobenzyl) oxy) benzaldehyde (2).

3.1.3. 2,3-bis(4-fluorobenzyloxy) benzaldehyde (3)

$C_{21}H_{16}F_2O_3$, m.p. (99-102) °C, (85%), color (grey), IR (cm^{-1}) str. 3050 (C-H), 2953 (C-H), 2720 -2820 (Aldehyde C–H), 1720 (C=O), 1600 (C=C), 1270 (C-O), 1150 (C-F), 850 (C-H). ^{1}H-NMR (ppm): 9.83 (1H, s, - CHO) 7.01-7.04 (3H, m, Ar-$H_{7,6,5}$), 7.05-7.08 (4H, m, Ar-$H_{10,11,14,13}$), 7.09- 7.48 (4H, m, Ar-$H_{17,18,21,20}$) 5.15, 5.20 (4H, s, CH_2*2) .^{13}C-NMR (ppm): 191.16: C_1, 176.55: C_{19}, 164.18: C_{12}, 161.69: C_2, 154.40: C_3, 132.57: C_4, 132.23: C_{16}, 130.77: C_9, 129.61: C_{14}, 129.53: C_{10}, 129.43: C_{17}, 129.35: C_{21}, 127.29: C_5, 116.11: C_7, 116.01: C_6, 115.90: C_{13}, 115.79: C_{18}, 113.40: C_{11}, 112.56: C_{20}, 70.72: C_{15}, 70.60: C_8. Figure 4 illustrates the confirmed structure of 1-(4-(4-fluorobenzyl) oxy-3-fluorophenyl)-3-phenylprop-2-en-1-one ($C_{21}H_{16}F_2O_3$) as established from the spectral characterization data.

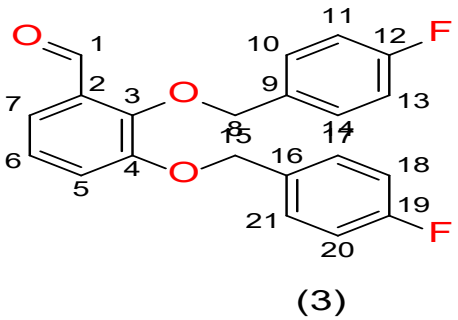

Figure 4: Structure of 2,3-bis(4-fluorobenzyloxy) benzaldehyde (3).

3.2. Characterization Results of Chalcone (4a and 4b)

3.2.1. (E)-1-(4-((4-fluorobenzyl) oxy) phenyl)-3-(m-tolyl) prop-2-en-1-one(4a)

$C_{23}H_{19}FO_2$, m.p. (176-179)°C, (75%), color (Light-yellow), IR (cm^{-1}) str. 3075 (C-H), 2916-2866 (C-H), 1653 (C=O), 1599 (C=C), 1228 (COC), 1012 (CF), 814 (CH).^{1}HNMR.(ppm): 8.03 (1H, d, βCH=), 7.77 (H, d, αCH=) 7.03-7.56 (12H, m, Ar-$H_{1,4,2,3,10,13,9,11,22,19,18,20}$) 5.11 (2H, s, O–$CH_2$Ph) 2.4 (3H, s, $ArCH_3$).^{13}CNMR(ppm): 188.81: C_{16}, 163.87: C_5, 162.30: C_8, 161.42: C_{15}, 144.24: C_6,143.59: C_{21} 140.96: C_{17}, 132.28: C_{19}, 131.98: C_{11}, 131.95: C_{13}, 131.53: C_3, 130.84: C_{12}, 130.77: C_{18}, 129.73: C_4, 129.53: C_{20}, 129.45: C_9, 128.46: C_{10}, 120.72: C_{14}, 115.79: C_2, 115.58:C_1, 114.62: C_{22}, 69.48: C_7, 21.6: C_{23}. Figure 5 illustrates the confirmed structure of the compound $C_{23}H_{19}FO_2$ as determined from the spectral characterization data.

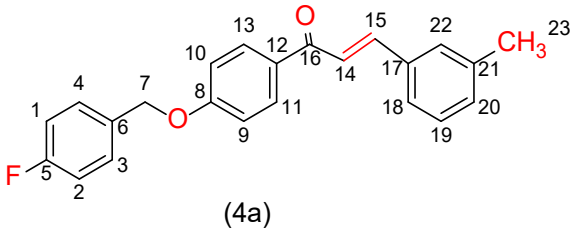

Figure 5: Structure of (E)-1-(4-((4-fluorobenzyl) oxy) phenyl)-3-(m-tolyl) prop-2-en-1-one(4a).

3.2.2. (E)-1-(4-(4-Fluorobenzyloxy) phenyl)-3-arylprop-2-en-1-one(4b)

$C_{23}H_{19}FO_2S$, m.p . (156-158)℃, 76%, color (yellow), IR (cm^{-1}) str. 3043 (C-H), 2916 (C-H), 1649 (C=C), 1220 (C-O-C), 818 (C-H), 619 (C-S), 1172 (C-F). ^{1}H-NMR. (ppm): 2.52 (3H, s, –S–CH_3), 5.11 (2H, s, O–CH_2– (benzylic)), 8.04 (1H, d, –CH= (β-proton)), 7.76 (1H, s, –CH= (α-proton)), 7.04-7.09 (4H, m, Ar-$H_{12,23,9,10}$)), 7.11-7.44 (4H, m, Ar-$H_{21,20,17,18}$), 7.48-7.57 (4H, m, Ar-$H_{1,6,3,4}$). ^{13}C-NMR (ppm): 188.89: C_{13}, 164.18: C_8, 162.63: C_2, 143.87: C_{19}, 142.43: C_{15}, 132.30: C_5, 132.27: C_{10}, 131.84: C_{11}, 131.86: C_4, 131.10: C_{23} ,129.77: C_{20}, 129.69: C_6, 129.06: C_{17}, 126.45: C_{16} ,126.30: C_{18}, 121.04: C_{14}, 116.07: C_9, 115.85: C_{21}, 114.96: C_1, 114.61: C_3, 112.39: C_{12}, 69.80: C_7, 15.48: C_{22}. Figure 6 illustrates the confirmed structure of the compound $C_{23}H_{19}FO_2S$ as determined from the spectral characterization data.

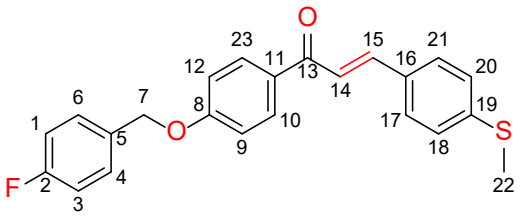

Figure 6: Structure of (E)-1-(4-(4-Fluorobenzyloxy) phenyl)-3-arylprop-2-en-1-one(4b).

3.3. Characterization Results of One-pot Synthesis of Pyrazolines

The characteristic ABX spin system of the pyrazoline ring (diastereotopic CH_2 protons, H_a and H_b, coupled to the methine H_x) was identified in all derivatives (5a–i). Detailed assignments correlating H_a, H_b, and H_x with their respective carbon is summarized in table S3 (Supplementary tables).

3.3.1. 5-(3-chlorophenyl)-3-(4-((4-fluorobenzyl) oxy) phenyl)-1-phenyl-4,5-dihydro-1H-pyrazole (5a)

$C_{28}H_{22}ClFN_2O$,m.p.(154-156)°C, (92)%, color (very light yellow), IR (cm^{-1}) str. 3039 (C-H), 2919-2871 (C-H), 1598 (C=N), 1500 (C=C), 1348 (CN), 1243 (COC), 1070 (CF), 742 (CCl), ^{1}HNMR(ppm): 3.07 (1H, dd, CH_2-Ha), 3.81 (1H, dd, CH_2-Hb), 5.06 (2H, s, Benzylic–CH_2–O–), 5.21 (1H, dd ,Hx) , 6.76-7.66 (17H, m, Ar-$H_{1,6,3,4,12,13,9,10,19,20,21,17,24,25,26,27,28}$) ^{13}C-NMR (ppm): 164.37: C_8, 161.92: C_2, 159.74: C_{14} , 147.23: C_5, 145.47: C_{23}, 141.78: C_{22}, 133.85: C_{19} 133.00: C_{18}, 132.97: C_{25}, 131.24: C_{24}, 130.03: C_{17}, 129.95: C_{11}, 129.93: C_{12}, 129.58: C_{26} ,128.38: C_6, 127.96: C_{10}, 127.88: C_{20}, 126.27: C_4, 119.71: C_{21}, 116.29: C_9, 116.08: C_{13}, , 115.7: C_3, 115.53: C_1,

113.84: C_{28},103.04: C_{27}, 69.96: C_7, 64.41: C_{16}, 44.26: C_{15}. Figure 7 illustrates the confirmed structure of the compound $C_{28}H_{22}ClFN_2O$ as established from the spectral characterization data.

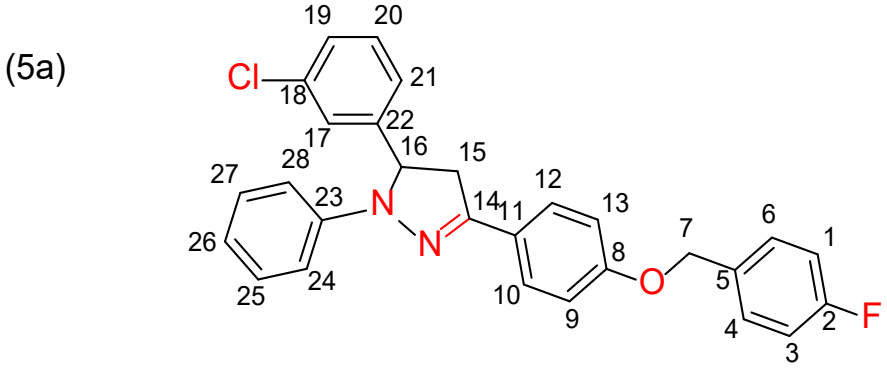

Figure 7: Structure of 5-(3-chlorophenyl)-3-(4-((4-fluorobenzyl) oxy) phenyl)-1-phenyl-4,5-dihydro-1H-pyrazole (5a).

3.3.2. 3-(4-((4-fluorobenzyl)oxy)phenyl)-1-phenyl-5-(m-tolyl)-4,5-dihydro-1H-pyrazole (5b)

$C_{29}H_{25}FN_2O$, m.p. (176-178) ℃, (88) %, color (very light yellow), IR (cm^{-1}) str. 3070-2927 (C-H), 2927 (C-H), 1594 (C=N), 1494 (C=C), 1427 (CH_3), 1380 (C-O-C), 1241 (C-F), 995 (N-N), 752 (C-H). ^{1}H-NMR (ppm): 2.65 (3H, s, Aromatic–CH_3), 3.16 (1H, dd, CH_2-Ha), 4.02 (1H, dd, CH_2-Hb), 5.22(2H, s, Ar-CH_2-O), 5.53 (1H, dd, Hx), 6.85-7.85 (17H, m, Ar-$H_{6,7,3,4,13,14,10,11,21,20,19,17,28,27,26,25,24}$). ^{13}CNMR (ppm): 164.72: C_5, 161.45: C_{24}, 159.58: C_{12}, 147.09: C_8, 145.58: C_{18}, 140.7: C_{17}, 137.69: C_{21}, 134.35: C_{20}, 132.97: C_2, 131.43: C_{28}, 129.97: C_{27}, 129.87: C_{26}, 129.49: C_9, 129.40: C_{19}, 128.63: C_4, 128.04: C_{14}, 127.87: C_{22}, 127.76: C_3, 127.42: C_7, 126.5: C_{10}, 119.32: C_{13}, 115.96: C_6, 115.44: C_{11}, 113.55: C_{29}, 106.31: C_{25}, 69.9: C_1, 62.17: C_{16}, 42.6: C_{15}, 20.09: C_{23}. Figure 8 illustrates the confirmed structure of the compound $C_{29}H_{25}FN_2O$ as established from the spectral characterization data.

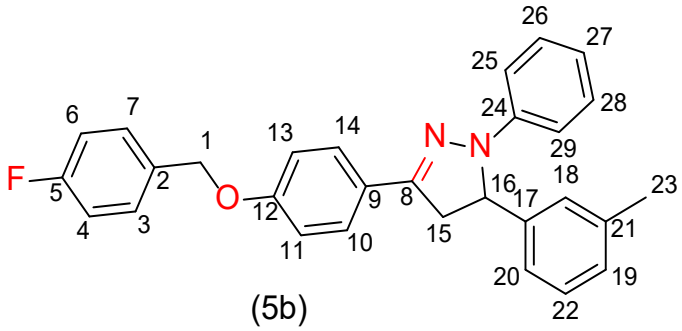

Figure 8: Structure of 3-(4-((4-fluorobenzyl) oxy) phenyl)-1-phenyl-5-(m-tolyl)-4,5-dihydro-1H-pyrazole(5b).

3.3.3. 3-(4-((4-fluorobenzyl) oxy)-3-methoxyphenyl)-5-(4-((4-fluorobenzyl) oxy) phenyl)-1-phenyl-4,5-dihydro-1H-pyrazole (5c)

$C_{36}H_{30}F_2N_2O_3$, m.p. (123-126°C), (90) %, color(yellow), IR (cm^{-1}) str. 3068 (C-H), 2931-2890 (C-H), 1511 (C=C), 1598 (C=N), 1226 (C-O), 1137 (C-F), 1000 (N-N), 755 (CH). ^{1}HNMR(ppm): 4.06 (3H, s, OCH_3), 3.21 (1H, dd, CH_2-Ha), 3.93 (1H , dd, CH_2-Hb), 5.21 (2H, s, -O-CH_2-), 5.30 (1H, dd, CH-Hx), 6.97-7.86 (21H, m, $ArH_{3,4,6,7,9,10,12,13,15,16,17,18,19,24,25,27,28,31,32,34,35}$), ^{13}CNMR(ppm): 164.28: C_{33}, 164.06: C_5, 161.00: C_{20}, 160.80: C_{26}, 159.17: C_{11}, 149.14: C_{14}, 148.34: C_{30}, 146.80: C_8, 145.26: C_{32}, 135.32: C_{23}, 132.61: C_{24}, 132.57: C_{31}, 132.51: C_{35}, 129.60: C_2, 129.52: C_7, 129.49: C_{13}, 129.41: C_{18}, 128.97: C_{17}, 127.32: C_{16}, 125.99: C_9, 122.17: C_3, 119.01: C_{19}, 118.91: C_{25}, 115.79: C_{28}, 115.56: C_{34}, 115.51: C_{10}, 115.28: C_{12}, 115.03: C_{27}, 113.36: C_{15}, 112.07: C_4, 111.71: C_6, 70.29: C_{29}, 69.45: C_{22}, 64.28: C_1, 56.07: C_{36}, 43.84: C_{21}. Figure 9 illustrates the confirmed structure of the compound $C_{36}H_{30}F_2N_2O_3$ as established from the spectral characterization data.

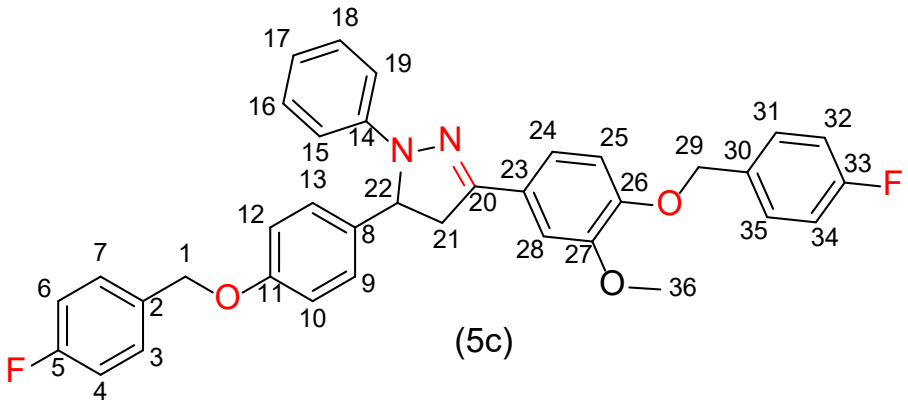

Figure 9: Structure of 3,5-bis(4-((4-fluorobenzyl) oxy) phenyl)-1-phenyl-4,5-dihydro-1H-pyrazole(5c).

3.3.4. 3-(4-((4-fluorobenzyl) oxy) phenyl)-5-(4-methoxyphenyl)-1-phenyl-4,5-dihydro-1H-pyrazole (5d).

$C_{29}H_{25}FN_2O_2$, m.p. (135-137°C), (90) %, color (light yellow), IR (cm^{-1}) str, 3050 (C-H), 2918-2871 (C-H), 1596 (C=N), 1513 (C=C), 1241 (C-F), 1177 (C-O), 1126 (N-N), 831 (CH). ^{1}HNMR (ppm): 3.11 (1H, dd, CH_2-Ha), 3.81 (1H, dd, CH_2-Hb), 5.08 (2H, s, -O-CH2-) 5.22 (1H, dd, CH-Hx), 6.73-7.7 (17H, m, $ArH_{2,3,4,5,6,8,9,11,12,18,19,21,22,25,26,28,29}$). ^{13}CNMR (ppm)**:** 43.90: C_{15}, 55.36: C_{13}, 64.07: C_{16}, 69.45: C_{23}, 113.36: C_{19}, 114.00: C_{26}, 114.58: C_{21},114.99: C_9, 115.50: C_{11}, 115.70: C_2, 118.88: C_6, 125.37: C_4, 126.08: C_{28}, 127.20: C_3, 127.31: C_{17}, 128.44: C_5, 128.96: C_{22}, 129.40: C_{25}, 129.51: C_{12},130.11: C_8, 130.71: C_{18}, 132.52: C_{29}, 134.86: C_7,141.79: C_{24}, 145.23: C_1, 146.73: C_{14}, 159.11: C_{10}, 161.00: C_{20}, 164.26: C_{27}. Figure 10 illustrates the confirmed structure of the compound $C_{29}H_{25}FN_2O_2$ as established from the spectral characterization data.

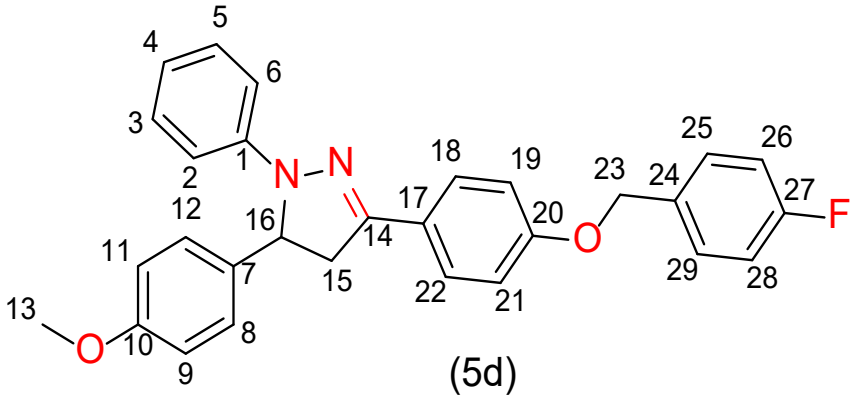

Figure 10: Structure of 3-(4-((4-fluorobenzyl) oxy) phenyl)-5-(4-methoxyphenyl)-1-phenyl-4,5-dihydro-1H-pyrazole (5d).

3.3.5. 3-(4-((4-fluorobenzyl) oxy) phenyl)-1-phenyl-5-(thiophen-2-yl)-4,5-dihydro-1H-pyrazole (5e)

$C_{26}H_{21}FN_2OS$, m.p. (145-146°C), (85) %, color (yellow), IR (cm^{-1}) str. 3120 (C-H), 2920-2869 (C-H), 1604 (C=N), 1440 (C=C), 1247 (C-O), 1172 (C-F), 900 (C-H), 700 (C-S). ^{1}H-NMR (ppm): 3.07 (1H, dd, CH_2-Ha), 3.61 (1H, dd, CH_2-Hb), 4.88 (2H, s, $PhCH_2O$), 5.31 (1H, dd, CH-CHx), 6.64-6.79 (3H, m, Thiophenering), 6.82-7.69 (13H, m, Ar-H). ^{13}CNMRppm: 44.21: C_{21},60.74: C_{22},69.50: C_1, 104.65: C_{10}, 113.88: C_{19}, 115.05: C_{15}, 115.12: C_4, 115.55: C_6, 115.84: C_{12}, 119.61: C_8, 124.22: C_{13}, 124.98: C_{26}, 125.83: C_9, 126.42: C_{16}, 126.71: C_{17}, 127.12: C_{18}, 127.34: C_{23}, 129.02: C_7, 129.21: C_{24}, 129.45: C_3, 129.60: C_2, 146.41: C_{25}, 147.40: C_{20}, 158.85: C_{14}, 159.32: C_{11}, 161.04: C_5. Figure 11 illustrates the confirmed structure of the compound $C_{26}H_{21}FN_2OS$ as established from the spectral characterization data.

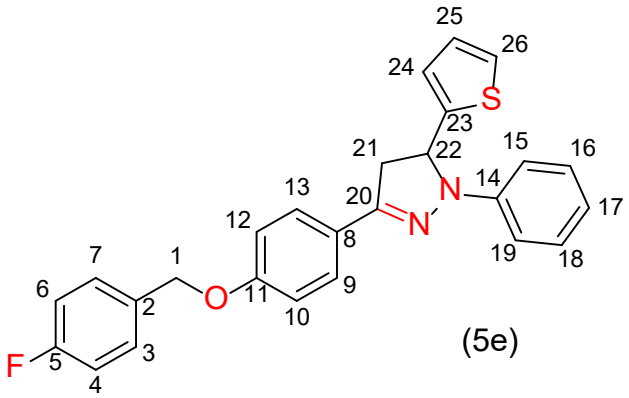

Figure 11: Structure of3-(4-((4-fluorobenzyl) oxy) phenyl)-1-phenyl-5-(thiophen-2-yl)-4,5-dihydro-1H-pyrazole (5e).

3.3.6. 5-(3,4-bis((4-fluorobenzyl) oxy) phenyl)-3-(4-((4-fluorobenzyl) oxy) phenyl)-1-phenyl-4,5-dihydro-1H-pyrazole (5f)

$C_{42}H_{33}F_3N_2O_3$, m.p. (143-145°C), (75%), color (yellow), IR (cm^{-1}) str. 3041 (C-H), 2924-2867 (C-H), 1598 (C=N), 1515 (C=C), 1229 (C–O–C), 1127 (C–F), 1004 (N–N), 830 (C–H). ^{1}HNMR (ppm): 3.01 (1H, dd, CH_2-Ha), 3.73 (1H, dd, CH_2-Hb), 5.00 (2H, s, CH_2O) ×3), 5.11 (1H, dd, CH-Hx), 6.76-7.65 (24H, m, Ar-$H_{3,4,6,7,9,10,12,13,15,16,17,18,19,25,26,28,29,31,35,34,38,39,41,42}$). ^{13}C-NMR ppm: 43.53: C_{21}, 63.95: C_{22}, 69.16: C_{23}, 70.20: C_{36}, 70.43: C_1, 93.13: C_{26}, 100.80: C_{25}, 103.84: C_{31}, 112.22: C_6, 113.04: C_{12}, 114.72: C_4,115.00: C_{41} 115.11: C_{10}, 115.21: C_{35}, 115.27: C_{19}, 115.32: C_{17}, 115.49: C_{15}, 118.74: C_{34}, 118.77: C_{28}, 125.62: C_7, 127.04: C_3, 128.69: C_{42}, 128.91: C_{13}, 128.99: C_8, 129.15: C_9, 129.23: C_{16}, 132.18: C_2, 132.39: C_{29}, 132.67: C_{18}, 134.77: C_{39}, 136.05: C_{30}, 144.93: C_{24}, 145.52: C_{14}, 147.88: C_{37}, 148.84: C_{38}, 158.87: C_{32}, 160.90: C_{20}, 161.11: C_{33}, 161.12: C_{11}, 163.35: C_{40}, 163.44: C_{27}, 163.56: C_5. Figure 12 illustrates the confirmed structure of the compound $C_{42}H_{33}F_3N_2O_3$ as established from the spectral characterization data.

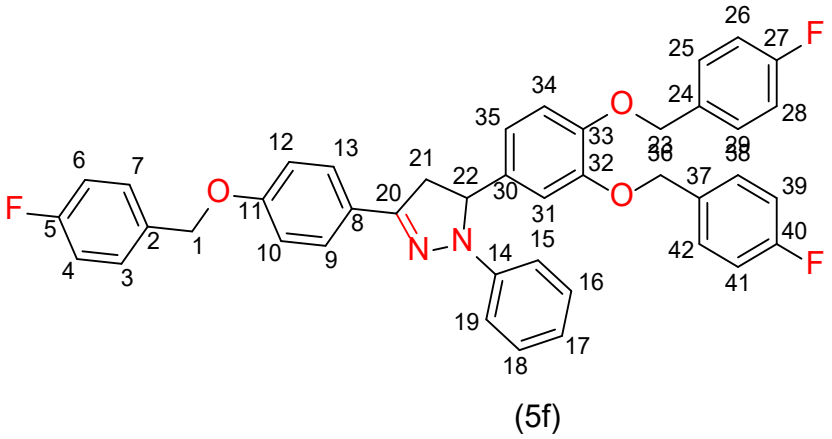

Figure 12: Structure of 5-(3,4-bis((4-fluorobenzyl) oxy) phenyl)-3-(4-((4-fluorobenzyl) oxy) phenyl)-1-phenyl-4,5-dihydro-1H-pyrazole(5f).

3.3.7. 5-(3-((4-fluorobenzyl) oxy) phenyl)-3-(4-((4-fluorobenzyl)oxy)phenyl)-1-phenyl-4,5-dihydro-1H-pyrazole (5g)

$C_{35}H_{28}F_2N_2O_2$, m.p .(143-145°C), (85)%, color (light yellow), IR (cm^{-1}) str. 3054 (C-H), 2892-2866 (C-H), 1505 (C=C), 1596 (C=N), 1224 (C-O-C), 1036 (C-F), 1315 (C-N), 822 (C-H), ^{1}HNMR (ppm): 3.08 (1H , dd, CH_2-Ha), 3.78 (1H, dd, CH_2-Hb), 4.98 (2H, s, OCH_2), 5.20 (1H, dd, CH-Hx), 6.75-7.67 (21H , m, Ar-$H_{3,4,6,7,9,10,12,13,15,16,17,18,19,24,25,27,28,31,33,34,35}$)· ^{13}C-NMRppm: 163.76: C_{26}, 161.32: C_5, 159.09: C_{11}, 158.04: C_{32}, , 147.61: C_{20}, 146.66: C_{14}, 145.17: C_{30} , 135.26:C_{23}, 132.7:C_2 , 132.67: C_3, 132.52: C_{13}, 129.43: C_9, 129.34: C_{34}, 128.91: C_{16}, 127.26: C_{17}, 127.17: C_{18} ,126.02: C_7, 125.40: C_{15}, 123.16: C_{24}, 121.73: C_{28}, 120.31: C_8 ,118.87: C_6 , 116.02: C_{31}, 115.68: C_4, 115.64: C_{12}, 115.47: C_{10}, 115.42: C_{35}, 115.38: C_{25}, , 114.96: C_{27}, 113.33: C_{33}, 106.79: C_{19}, 72.72: C_{29},

69.40: C_1, 63.98: C_{22}, 43.82: C_{21}. Figure 13 illustrates the confirmed structure of the compound $C_{35}H_{28}F_2N_2O_2$ as established from the spectral characterization data.

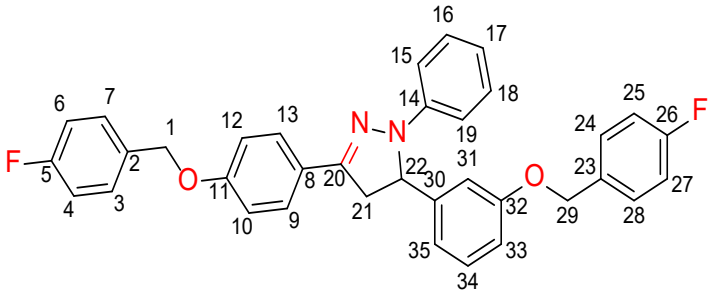

(5g)

Figure 13: Structure of 5-(3-((4-fluorobenzyl) oxy) phenyl)-3-(4-((4-fluorobenzyl) oxy) phenyl)-1-phenyl-4,5-dihydro-1H-pyrazole(5g).

3.3.8. 3-(4-((4-fluorobenzyl) oxy) phenyl)-5-(3-(methylthio) phenyl)-1-phenyl-4,5-dihydro-1H-pyrazole (5h)

$C_{29}H_{24}FNOS$, m.p. (143-145) ℃, (94)%,color(yellow), IR (cm^{-1}) str. 3050(C-H), 2950-2850(C-H), 1585(C=N), 1450(C=C), 1250(C–O–C), 1170(C–F), 1030(N-N), 700(C-S), 850(CH).^{1}HNMR (ppm): 2.46 (3H, s, SCH_3), 3.08(1H, dd, CH_2-Ha), 3.79(1H ,dd , , CH_2-Hb),5.05(2H,s, O–CH_2–), 5.22(1H, dd, CH-Hx), 6.75-7.67(17H,m,Ar-$H_{3,4,6,7,9,10,12,13,15,16,17,18,19,24,26,27,28}$),^{13}C-NMR(ppm): 15.93:C_{29}, 43.85:C_{21}, 64.22:C_{22}, 69.52:C_1, 112.50:C_9, 113.43:C_6, 115.08:C_{15}, 115.58:C_{12}, 115.79:C_4, 117.66:C_{19}, 119.08:C_{17}, 119.82:C_{24}, 126.02:C_7, 126.61:C_3, 127.36:C_{27}, 127.37:C_{13}, 128.88:C_{28}, 129.04:C_{10}, 129.43:C_8, 129,52:C_{18}, 132.61:C_2, 137.78:C_{16}, 139.71:C_{26}, 145.19:C_{14}, 146.77:C_{23},151.68:C_{20}, 159.23:C_{25}, 161.46ppm:C_{11}, 163.91ppm:C_5. Figure 14 shows the structure of the compound $C_{29}H_{24}FNOS$.

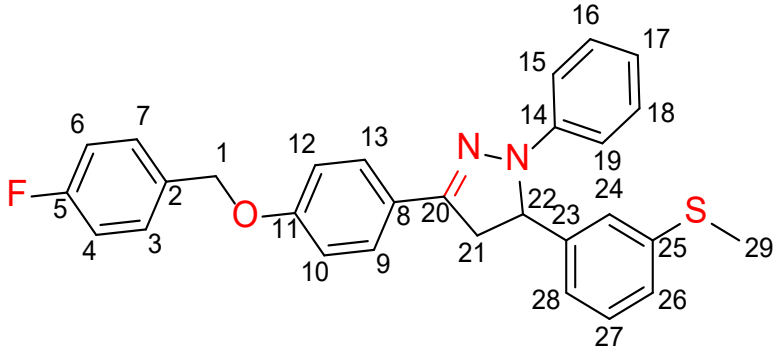

Figure 14: Structure of 3-(4-((4-fluorobenzyl)oxy)phenyl)-5-(3-(methylthio)phenyl)-1-phenyl-4,5-dihydro-1H-pyrazole(5h).

3.3.8. 3-(4-((4-fluorobenzyl)oxy)phenyl)-1-phenyl-5-(p-tolyl)-4,5-dihydro-1H-pyrazole (5i)

$C_{29}H_{25}FN_2O$, m.p. (152-154℃), (94) %, color (light pink), IR (cm^{-1}) str. 3075 (C-H), 2921-2873 (C-H), 1495 (C=C), 1596 (C=N), 1243 (C-F), 1176 (C-O-C), 1066 (N-N), 995 (C-H). ^{1}H-NMR (ppm): 2.43 (3H, s, CH_3), 3.19 (1H, dd, CH_2-Ha), 3.89 (1H, dd, CH_2- Hb), 5.17 (2H, s, CH_2–O(benzylic), 5.31 (1H, dd, CH-Hx), 6.85-7.79 (17H, m, Ar-$H_{3,6,5,7,10,11,12,13,14,18,19,21,22,25,26,29,28}$). ^{13}C-NMRppm: 21.29: C_8, 44.27: C_{16}, 64.72: C_1, 69.81: C_{23}, 113.70: C_{26}, 115.35: C_{11}, 115.58: C_{14}, 115.86: C_{28},116.15: C_{10}, 119.24: C_{12}, 126.28: C_{18},126.43: C_3, 127.68: C_{24}, 128.32: C_{17}, 129.08: C_{13}, 129.33: C_{22}, 129.56: C_6, 129.78: C_5, 129.88: C_{29}, 129.96: C_{21}, 130.24: C_{25}, 132.94: C_7, 137.64: C_4, 140.21: C_2, 145.61: C_9, 147.13: C_{15}, 159.48: C_{19}, 161.36: C_{20}, 164.63: C_{27}. Figure 15 illustrates the confirmed structure of the compound $C_{29}H_{25}FN_2O$ as established from the spectral characterization data.

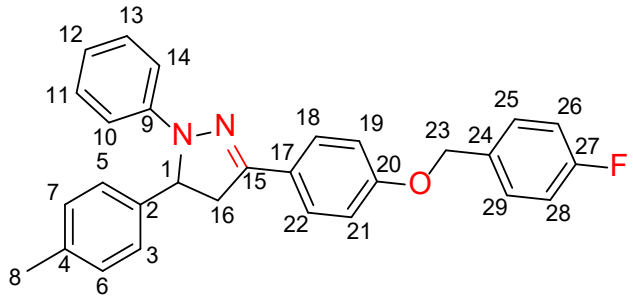

Figure 15: Structure of 3-(4-((4-fluorobenzyl) oxy) phenyl)-1-phenyl-5-(p-tolyl)-4,5-dihydro-1H-pyrazole (5i).

3.4. Characterization Results of Two pot Synthesis of Pyrazolines

3.4.1. 3-(4-((4-fluorobenzyl) oxy) phenyl)-5-(3-(methylthio) phenyl)-1-phenyl-4,5-dihydro-1H-pyrazole

$C_{29}H_{24}FNOS$, m.p. (143-145) ℃, (88) %, color(yellow), spectra are the same as one-pot synthesis.

3.4.2. 3-(4-((4-fluorobenzyl)oxy)phenyl)-1-phenyl-5-(p-tolyl)-4,5-dihydro-1H-pyrazole

$C_{29}H_{25}FN_2O$, m.p. (152-154) ℃, (85) %, color (light pink), spectra are the same as one-pot synthesis.

3.5. Evidence of Successful Synthesis and Transformation

As shown in figure 16 the FT-IR spectra comparison of benzyloxy, chalcone, and pyrazoline compounds, illustrating their characteristic absorption bands. Distinct peaks indicate structural differences among the three compounds. Table 1 compares the yields and melting points of compounds 5h and 5i synthesized by one-pot and two-pot methods. The one-pot route provided higher yields (94%) than the two-pot method (85–88%), while both methods produced compounds with identical melting points.

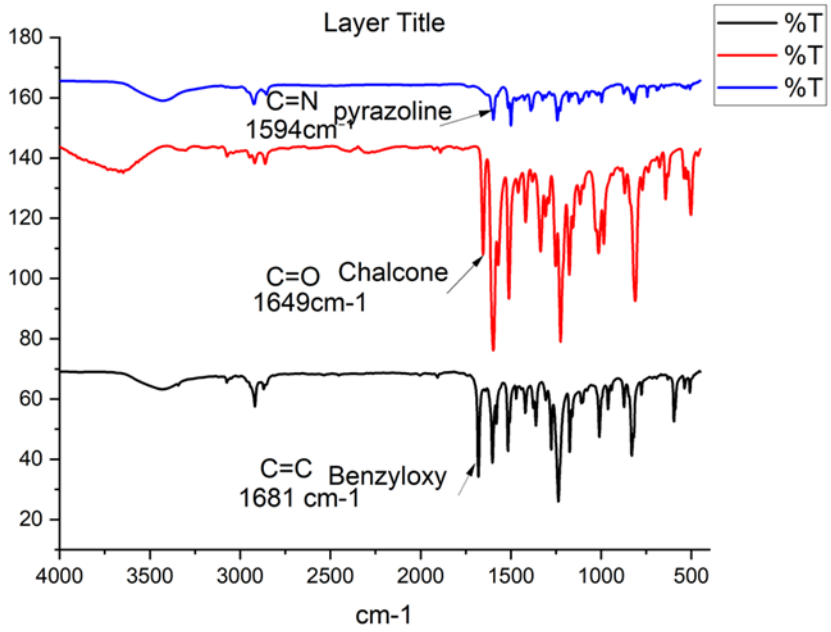

Figure 16: The FT-IR characteristic comparison among Benzyloxy, Chalcone and Pyrazoline compound.

Table 1: Comparative yields of compounds 5h and 5i obtained via one-pot and two-pot methods.

Compound	Route	Theoretical (0.002 moL)	Isolated mass (g)	Isolated (mmoL)	Yield (%)	m.p. (°C)
5h ($C_{29}H_{24}FNOS$, 441.56 g/moL)	One-pot	0.88 g	0.83 g	1.88	94	143–145
5h ($C_{29}H_{24}FNOS$, 441.56 g/moL)	Two-pot	0.88 g	0.77 g	1.75	88	143–145
5i ($C_{29}H_{25}FN_2O$, 424.51 g/moL)	One-pot	0.85 g	0.81 g	1.90	94	152–154
5i ($C_{29}H_{25}FN_2O$, 424.51 g/moL)	Two-pot	0.85 g	0.72 g	1.70	85	152–154

3.6. Antibacterial Activity

Table 2 shows the antibacterial activity reported as inhibition zone diameters (mm, mean ± SD) for compounds 5a–5i and 4a at 200–800 ppm. Assay: agar disc-diffusion; DMF served as the solvent-only control and showed no inhibition zone across all concentrations. against *E. coli*. Raw replicate inhibition zone diameters (mm) of chalcone and pyrazoline derivatives illustrated in table S1. Statistical analysis of *E. coli* using one-way ANOVA ($F = 842.6$, $p < 0.0001$) and Tukey's test revealed significant differences among the tested compounds. The values of the inhibition zone ranged between 0.0 and 20.0 mm, 0.0 and 24.3 mm, 0.0 and 33.4 mm, and 0.0 and 35.0 mm for the concentrations of 200, 400, 600, and 800 ppm, respectively. The largest inhibition zones were exhibited by 5d (20.0 mm) at 200 ppm, 5a (24.3 mm) at 400 ppm, 5c (33.4 mm) at 600 ppm, 5a (35.0 mm), and 5c (35.0 mm) at 800 ppm. These compounds displayed to have superior efficacy of inhibition relative to the standard antibiotic amoxicillin.

Table 2: Antibacterial activity of 5a–5i and 4a at 200–800 ppm against *E. coli*.

NO.	200 ppm (mm)	400 ppm (mm)	600 ppm (mm)	800 ppm (mm)
DMF	0.0 ^{d}	0.0 ^{g}	0.0 ^{e}	0.0 ^{f}
5a	0.0 ^{d}	24.3±0.6 ^{a}	32.1 ± 0.5 ^{a}	35.0 ± 0.7 ^{a}
5b	10.2 ± 0.5 ^{c}	16.0 ± 0.6 ^{c}	10.1 ± 0.3 ^{d}	8.0 ± 0.4 ^{e}
5c	0.0 ^{d}	20.2 ± 0.4 ^{b}	33.4 ± 0.8 ^{a}	35.0 ± 0.9 ^{a}
5d	20.0 ± 0.5 ^{a}	21.1 ± 0.7 ^{b}	21.0 ± 0.6 ^{b}	23.0 ± 0.8 ^{c}
5e	17.0 ± 0.4 ^{b}	5.0 ± 0.2 ^{f}	0.0 ^{e}	18.0 ± 0.5^{d}
5f	0.0 ^{d}	12.2 ± 0.3 ^{d}	13.0 ± 0.4 ^{c}	33.0 ± 0.8 ^{b}
5g	0.0 ^{d}	8.1 ± 0.2 ^{e}	22.0 ± 0.6 ^{b}	31.0 ± 0.7 ^{b}
5h	0.0 ^{d}	0.0 ^{g}	0.0 ^{e}	0.0 ^{f}
5i	0.0 ^{d}	0.0 ^{g}	10.0 ± 0.3 ^{d}	21.0 ± 0.6 ^{c}
4a	0.0 ^{d}	0.0 ^{g}	0.0 ^{e}	8.0 ± 0.4 ^{e}
Amoxicillin	10.0 ± 0.3 ^{c}	13.0 ± 0.4 ^{d}	15.0 ± 0.5 ^{c}	18.0 ± 0.5 ^{d}
ANOVA p-value	< 0.0001	< 0.0001	< 0.0001	< 0.0001

0 = No inhibition zone observed (no detectable antibacterial activity at the tested concentration). Values represent mean ± SD of three independent replicates (n = 3). DMF= N, N-dimethylformamide (negative control). Superscript letters (a, b, c, etc.) in each column indicate Tukey's HSD post-hoc groupings. Means with different letters differ significantly ($p < 0.05$).

Table 3 shows the antibacterial activity reported as inhibition zone diameters (mm, mean ± SD) for compounds 5a–5i and 4a at 200–800 ppm. Assay: agar disc-diffusion; DMF served as the solvent-only control and showed no growth across all concentrations. against *S. aureu*s. Raw replicate inhibition zone diameters (mm) of chalcone and pyrazoline derivatives illustrated in table S2. Significant different between the investigated compounds were found by statistical analysis of *S. aureu*s using one-way ANOVA ($F = 424.8$, $p < 0.0001$) and Tukey's test. For concentrations of 200, 400, 600, and 800 ppm, the inhibition zone values varied between 0.0 and 22.0 mm, 0.0 and 33.0 mm, 0.0 and 35.0 mm, and 0.0 and 38.0, respectively. The reproducible inhibition trends across all concentrations confirmed the robustness of the results and emphasized the superior efficacy of the pyrazoline derivatives relative to the standard antibiotic amoxicillin. Compounds 4a (22.0 mm) at 200 ppm, 4a (33.0 mm) at 400 ppm, 5c (35.0 mm) at 600 ppm, and 5c (38.0 mm) at 800 ppm were shown the superior efficacy of inhibition relative to the standard antibiotic amoxicillin.

Table 3: Antibacterial activity of 5a–5i and 4a at 200–800 ppm against *S. aureu*s.

NO.	200 ppm (mm)	400 ppm (mm)	600 ppm 9mm)	800 ppm (mm0
DMF	0.0 ^{c}	0.0 ^{e}	0.0 ^{f}	0.0 ^{e}
5a	0.0 ^{c}	24.0 ± 0.6 ^{b}	32.0 ± 0.7 ^{b}	35.0 ± 0.8 ^{a}
5b	0.0 ^{c}	25.0 ± 0.7 ^{b}	26.0 ± 0.6 ^{c}	0.0 ^{e}
5c	0.0 ^{c}	0.0 ^{e}	35.0 ± 0.9 ^{a}	38.0 ± 1.0 ^{a}

Table 3: continue				
5d	0.0 [c]	0.0 [e]	24.0 ± 0.6 [c]	34.0 ± 0.8 [b]
5e	0.0 [c]	0.0 [e]	20.0 ± 0.5 [d]	30.0 ± 0.7 [c]
5f	0.0 [c]	23.0 ± 0.6 [c]	25.0 ± 0.7 [c]	30.0 ± 0.9 [c]
5g	12.4 ± 0.5 [b]	12.3 ± 0.5 [d]	12.2 ± 0.4 [e]	12.0 ± 0.4 [d]
5h	0.0 [c]	0.0 [e]	0.0 [f]	0.0 [e]
4a	22.0 ± 0.7 [a]	33.0 ± 0.8 [a]	34.0 ± 0.9 [a]	35.0 ± 0.8 [a]
5i	0.0 [c]	0.0 [e]	0.0 [f]	20.0 ± 0.6 [d]
Amoxicillin	20.0 ± 0.6 [a]	23.0 ± 0.7 [c]	29.0 ± 0.8 [b]	30.0 ± 0.9 [c]
ANOVA p-value	< 0.0001	< 0.0001	< 0.0001	< 0.0001

0 = No inhibition zone observed (no detectable antibacterial activity at the tested concentration). Values represent mean ± SD of three independent replicates (n = 3). DMF= N, N-dimethylformamide (negative control). Superscript letters (a, b, c, etc.) in each column indicate Tukey's HSD post-hoc groupings. Means with different letters differ significantly ($p < 0.05$).

4. Discussion

4.1. Chemistry

This study utilized both the conventional stepwise method and the one-pot procedure to synthesize novel pyrazoline derivatives. The classical method was utilized to synthesize two α, β-unsaturated chalcones (4a and 4b) through the reaction of benzyloxy acetophenone with substituted aromatic aldehydes. The chalcones were then cyclized with phenyl hydrazine, resulting in the formation of two novel pyrazolines (5h and 5i). The one-pot method involved the direct condensation of benzyloxy acetophenone with substituted benzaldehydes, followed by the addition of phenyl hydrazine, resulting in a series of pyrazoline derivatives (5a–g). In comparison to the classical approach, the one-pot strategy demonstrated greater simplicity, reduced time requirements, and yielded higher outputs, although both methods ultimately achieved the target compounds with relatively high overall yields. Scientists use one-pot along with two-pot methods to create pyrazoline derivatives, but the choice between these methods depends on the type and purpose of reactants. During one-pot synthesis, all the starting materials, including an aromatic aldehyde and a ketone like acetophenone, are introduced directly to a single reaction vessel with hydrazine derivatives, where multi-phase reactions proceed without intermediate separation [88]. The one-pot synthesis produces better results since it combines advantages of operational ease and short reaction times while needing low solvent amounts and resulting in high yields, providing both environmental preservation and economic benefits. The control over individual reaction stages during condensation synthesis is restricted and causes side products to form when dealing with sensitive or multifunctional starting materials. The two-pot synthesis method executes chalcone intermediate production through Claisen–Schmidt condensation, followed by intermediate isolation before combining it with hydrazine derivatives to generate the desired pyrazoline. The two-pot synthesis method requires additional time and manual work for intermediate purification and individual reaction processes yet provides better reaction control together with higher selectivity and purer reaction outcomes [89]. The production process using one-pot synthesis is simpler than two-pot synthesis, but two-pot synthesis becomes essential for achieving better product purity or structural complexity in specific applications [90].

Chalcones serve as α, β-unsaturated ketones that work as important intermediates in organic synthesis to make starting materials for creating different heterocyclic compounds. The synthesis of pyrazoline derivatives through chalcones using hydrazine or substituted hydrazine follows a Michael addition step before ring formation takes place to produce the final pyrazoline structure. The reaction has gained popularity because it produces diverse biologically active compounds efficiently through its simple and effective process [91]. Chalcones can be used as starting materials to produce flavones, flavanones, aurones, and benzothiazepines alongside pyrimidines when reaction conditions and reagents vary. The multiple operational possibilities, coupled with their reactive enone structure position, position chalcones as key organic compounds for developing functional medical compounds and performing synthetic organic research for antimicrobial treatments and anti-inflammatory agents, as well as

anticancer medications and antioxidant-defense elements. The skeletons of these new derivatives of pyrazolines were consistent with the proposed structures based on physical properties and spectroscopic methods (FTIR, ^{1}H-NMR, and ^{13}C-NMR).

4.2. Spectroscopic Characterization

FTIR, ^{1}H NMR and ^{13}C NMR spectroscopy were used to characterize the synthesized chalcones and pyrazole derivatives. The FTIR spectra revealed the presence of typical functional groups, and the spectra obtained with the help of the method of the ^{1}H NMR and ^{13}C NMR were the detailed information about the aromatic, olefinic, and heterocyclic protons and carbons. The chemical shifts, coupling constants and multiplicities that were observed were entirely consistent with the proposed structure, and this indicated that all derivatives were successfully prepared. Despite the fact that the concept of conducting the mass spectrometric analysis is good and was recommended in the review, the procedure was not implemented in this revision because of the limitations and time constraints in the lab. However, FTIR, ^{1}H NMR, and ^{13}C NMR characterized rigorously all synthesized derivatives and are used in combination to give comprehensive structural validation. This is because the successful synthesis is justified by the congruence of the chemical shifts, coupling constants and functional group absorptions. Further, the synthetic methodology used (stepwise and one-pot) of these specific derivatives has not been reported in the past, thus highlighting the novelty of this work.

The FT-IR spectrum of the first compound revealed characteristic absorptions, with the lack of the wide band associated with the hydroxyl (OH) group in the 3400–3100 cm^{-1} range. This disappearance, resulting from substitution of the hydroxyl hydrogen with a benzyl group, confirms the successful formation of the compound [92]. The two specific peaks that clarify powerful evidence for the formation of the compound are the two bands present at the (2919-2863 cm^{-1}) region of (-CH_2-) in benzyloxy. A prominent absorption band at 1681 cm^{-1} was attributed to the stretching vibration of the carbonyl (C=O) group, while a prominent band found at (1600) cm^{-1} corresponds to the stretching of the carbon–carbon double bond (C=C); further peaks at (3066) cm^{-1} are indicative of sp^2 hybridized (C-H) stretching in aromatic compounds, (1417) cm^{-1} is CH_2 bending, (1357) cm^{-1} is CH_3 Bending, and the band (1010 cm^{-1}) shows C-F bending [93]. The ^{1}H-NMR spectrum confirmed the structure. The absence of the singlet at (13.15) ppm, which corresponds to the hydroxyl proton, indicates the substitution of the hydrogen atom with the protective group. A singlet was detected at (5.09) ppm, indicative of the benzylic –CH_2–O– group. The singlet at (2.55) ppm, attributed to the methyl (CH_3–CO) group, is slightly deshielded due to the influence of oxygen. Aromatic protons on the acetophenone ring, forming an AA′BB′ system, are expected to appear as two doublets in the region of (7.95, 7.93, 7.43, 7.39 ppm), integrating for two protons. The protons of the fluorinated benzyl ring (4-fluorobenzyl) are anticipated to give rise to a more complex splitting pattern, likely appearing as multiplets or within the (6.98, 7.00, 7.08, 7.11 ppm) range, because of long-range proton–fluorine coupling. This unique splitting helps support that the compound contains the fluorinated aromatic system [94]. Although the ^{13}C-NMR spectrum of the compound presents a unique signal that is observed for each carbon type, a singlet peak at (196) ppm corresponds to the carbonyl (C=O), a doublet signal at 163/162 ppm is attributed to the aromatic C–F split. A singlet peak at (161) ppm is attributed to electron-rich aromatic C–O bonds resulting from the presence of oxygen. Six singlets were observed, including a singlet peak at (69) ppm, which is attributed to the benzylic –CH_2–O– group (C10). Deshielded by oxygen, a singlet at (26) ppm was observed, corresponding to the methyl group (CH_3–CO) at C2, adjacent to the carbonyl carbon [95].

The FT-IR spectra of chalcone derivatives (4a and 4b) displayed distinct absorption peaks. A prominent band identified at (1650–1665) cm^{-1} was ascribed to the stretching vibration of the carbonyl (C=O) group. This frequency appears at a lower value compared to the typical carbonyl absorption (~1675 cm^{-1}), which can be explained by conjugation with the adjacent C=C double bond (enone system). Such conjugation leads to partial enolate character and reduces the bond order, thereby shifting the band to a lower wavenumber [96]. Additionally, absorption bands at (1250–12800 cm^{-1} were assigned to C–O stretching vibrations.

The ^{1}H-NMR spectrum displays several different signals that indicate the structural features of the compound. A singlet at (5.11) ppm corresponds to the two protons of the methylene group in the

benzyloxy moiety [97]. The compound (4a) in the (8.03) ppm and the alpha proton in the 7.77 ppm are observed to give a doublet. The single-point interaction between the two signals has a vicinal coupling constant of J = 15.5 Hz, a characteristic of a trans (E) configuration [98]. Past research indicated that $^{3}J(H\alpha H_2)$ values of chalcones of 15-16 Hz are only E-isomers and Z-isomers have weaker couplings (< 12 Hz). Both demonstrate a significant coupling constant, thereby confirming the (E)-configuration of the double bond [99]. For the compound (4b) the C=C geometry was assigned as E. The β-olefinic resonance appears as a pair of doublets at δ 7.8095/7.7706 ppm with $^{3}JH\alpha$–Hβ=15.57Hz (400 MHz, $CDCl_3$), diagnostic of a trans relationship in α, β-enones; the complementary α-olefinic signal is partially overlapped, giving an apparent smaller splitting (8.76 Hz). These values are fully consistent with literature ranges for trans vs cis alkenes and with reported chalcone precedents [100]. Olefinic region of the ^{1}H NMR spectrum (400 MHz, $CDCl_3$) of the representative chalcone (4a) derivative is shown in figure S1 and Olefinic region of the ^{1}HNMR spectrum (400 MHz, $CDCl_3$) of the chalcone (4b) derivative is shown in figure S2.

The ^{13}C-NMR spectrum of the compound is expected to exhibit separate signals from its structural fragments. The conjugated carbonyl carbon (C=O) of the enone system is the most deshielded signal and is usually found at 188.89 ppm (C_{13}) [101]. The α, β-carbon of the α, β-unsaturated ketone, the α carbon, appears at around 121.04 ppm (C_1) and the β carbon at 148.87 ppm (C_{14}) (alpha-carbon), with the beta-carbon more deshielded because of the direct conjugation with the carbonyl group. The benzylic methylene carbon (–OCH_2) attached to the 4-fluorobenzyl ether resonates at 69.80 ppm (C_7), with both the ether oxygen and the neighboring aromatic ring causing a downfield shift in the ^{13}C-NMR [102].

The FT-IR spectra of pyrazoline derivatives provide two strong indicators of pyrazoline formation: the initial aspect is the elimination of the carbonyl group in the compounds within the region of 1652-1660 cm^{-1}. Secondly, the prominent absorption band observed at 1594–1597 cm^{-1} was ascribed to the imine (C=N) stretching vibration, hence validating the creation of the pyrazoline ring system. The absence of the aliphatic absorption peak of (C=C) in the range of (1640-1680 cm^{-1}) is observed when comparing benzyloxy and chalcone.

Expectations for the ^{1}H-NMR in $CDCl_3$ were derived from the structural features of 3-(4-((4-fluorobenzyl) oxy) phenyl)-1,5-diphenyl-4,5-dihydro-1H-pyrazole. It contains a dihydropyrazole and two aromatic substituents at positions 1 and 5, together with a para-substituted phenyl group at position 3, linked via an ether bond to a para-fluorobenzyl moiety. The ^{1}H NMR spectra validated the existence of the 2-pyrazoline ring, evidenced by three doublet of doublets (dd) signals at 3.05, 3.70, and 5.00 ppm, corresponding to protons Ha, Hb, and Hx, respectively. These signals constitute an ABX spin system, indicative of two geminal protons and one vicinal proton [103]. The absence of signals for hydrazine or alkene protons (CH=CH) indicates successful cyclization. The protons of the para-fluorobenzyl ring may appear as doublets or even as two doublets due to fluorine-proton coupling and this pattern implies the position of the fluorine atom. The general spectral evidence should confirm the existence of a triaryl-substituted dihydropyrazole system and a para-substituted fluorobenzyl ether group, which is the suggested molecular structure. Correlation of ABX protons (H_a, H_b, H_x) with their corresponding carbons for pyrazoline derivatives 5a–5i, based on exact 13C chemical shifts from the characterization data is shown in table S3.

Performance of a ^{13}C-NMR in $CDCl_3$ is expected to record the structure based on the compound that includes the triaryl-substituted 4,5-dihydro-1H-pyrazole core and the para-fluorobenzyl ether substituent. The ^{13}C NMR spectra exhibited two discrete signals at 43.53 and 63.95 ppm, corresponding to the –CH_2– and –CH– carbons of the pyrazoline ring. The signals of sp^2-hybridized carbons (C=O, C=N, and C=C), usually seen in the 160–190 ppm region, were conspicuously lacking in the product spectrum [104]. This disappearance confirms that the compound has undergone cyclization and conversion to a saturated pyrazoline structure [105]. All characterizations can be shown in the supplementary figures (Figures S3-S41).

The FTIR spectra clearly show how specific functional groups evolve through the reaction sequence. In organic synthesis, such systematic spectral changes are one of the strongest indicators that each step occurred as planned. In the benzyloxy compound, the prominent C=C stretch at 1681 cm^{-1}

confirms the presence of a conjugated double bond or aromatic ring system. In the chalcone, this band shifts and a new strong C=O stretch at 1649 cm^{-1} appears. The carbonyl band is characteristic of an α, β-unsaturated ketone, which defines the chalcone structure. This proves that the Claisen–Schmidt condensation (between an aromatic aldehyde and acetophenone derivative) took place successfully. Finally, in the pyrazoline, the C=O absorption disappears, and a new band at 1594 cm^{-1} appears, assigned to C=N stretching. This is diagnostic for azomethine linkages in heterocyclic compounds like pyrazolines. Thus, the disappearance of the C=O and appearance of C=N serve as spectroscopic evidence for successful ring closure (cyclization). The characteristic comparison between Benzyloxy, Chalcone and pyrazoline can be shown in figure 16. Table 1 compares the yields and melting points of compounds 5h and 5i synthesized using one-pot and two-pot methods .For compound 5h ($C_{29}H_{24}FNOS$), the one-pot route produced a slightly higher yield (94%) than the two-pot route (88%) with the same melting point (143–145 °C).For compound 5i ($C_{29}H_{25}FN_2O$), the one-pot route also gave a better yield (94%) compared to the two-pot (85%) while maintaining the same melting point (152–154 °C).Overall, the one-pot synthesis proved more efficient, giving higher yields and comparable purity (as reflected by identical melting points) for both compounds.

4.3. Antibacterial Activity

The antibacterial efficacy of the synthesized chalcone and pyrazoline derivatives was assessed against *E. coli* and *S. aureus* through the disc diffusion method, utilizing concentrations from 200 to 800 ppm. The concentration level in the current investigation was started at 200 ppm. This choice was guided by initial screening at low levels (50 and 100 ppm) which always provided no observable zones of inhibition of the organisms being tested. The key assays were then done at concentrations of 200 ppm and above because any lower concentration would have been indistinguishable as negative growth controls and hard to replicate. It was at this level that the compounds started to demonstrate detectable antibacterial activity and permitted assessment of their effectiveness with a greater degree of reliability and evaluation of the trends of their concentration dependence in a more credible way. Results are expressed as inhibition zone diameters (mm); "0" denotes no inhibition zone observed.

The data revealed significant variations in the inhibition zones across different compounds and concentrations, suggesting a structural dependency and bacterial sensitivity to the compounds. The pyrazoline derivatives showed good antimicrobial action against *E. coli*, whereas the chalcone precursor (compound 4a) exhibited poor activity, producing only an 8 mm zone at the maximum concentration evaluated. Compound 5c had the highest activity, demonstrating a maximal inhibition zone of 35 mm at a concentration of 800 ppm. Compound 5f displayed the second-highest activity (33 mm), and 5g ranked third (31 mm). These compounds showed a clear dose-dependent effect, with little or no inhibition at lower doses but marked activity at higher concentrations. By contrast, compound 5h was completely inactive (0 at all concentrations), while compound 5i was only weakly active, producing inhibition zones at 600 and 800 pp. Overall, the compounds demonstrated greater efficacy against *S. aureus* than *E. coli*, consistent with the known vulnerability of Gram-positive bacteria due to their simpler cell wall structure [106]. Compound 5c produced the largest inhibition zone (38 mm at 800 ppm), followed by 5a (35 mm) and 5f (30 mm). Compound 5d exhibited moderate but consistent activity across concentrations (15–30 mm), while compound 5h was inactive against *E. coli* and also toward *S. aureus* at all ranges. Chalcone 4a again showed poor activity, with only 10 mm at the highest dose. Taken together, these findings support the conclusion that pyrazoline cyclization significantly enhances antibacterial activity, particularly against Gram-positive *S. aureus*.

The inhibition zone diameters (mm, mean ± SD) for compounds 5a–5i and 4a at 200–800 ppm has been illustrated in tables 2 and 3. The existence of electron- giving or electron-removing substituents seems to influence bioactivity, and activity generally increased in a dose-dependent manner. Since disc diffusion is diffusion- and solubility-limited, zone size is not linearly related to disc load; plateaus and shallow intermittent inversions can be expected with high loading because of a lack of diffusion/precipitation at the disc boundary. Our repeated runs ensured that we had reproducibility with acceptable variance. We then considered small non-monotonic deviations, following the rounding up to the nearest mm and validation by statistics, as method consistent deviations and not transcriptional. This is in

line with known models of diffusion and reported paradoxical high dose effects in antimicrobial testing [107]. The representative inhibition patterns of pyrazoline derivatives and chalcone illustrated in figure S42.

5. Conclusions

In view of the increasing antimicrobial resistance, this study was carried out to address the urgency of developing new antibacterial agents to counteract the effect. The objective was to summarize and describe a novel series of fluorinated pyrazoline-based ethers using both one-pot and stepwise synthesis methods, and to evaluate their antibacterial effectiveness. To deliver this, a strategic synthesis has been undertaken that commenced with the Claisen-Schmidt condensation to form chalcones and thence the cyclization with phenyl hydrazine to produce pyrazolines. The synthesis procedure was perfectly performed via both classical two-pot and eco-friendly one-pot protocols, with the latter providing a significantly greener product efficiency, ease of operation, and sustainability.

All the synthesized compounds were confirmed through structural characterization with the help of FTIR, ^{1}H-NMR, and ^{13}C-NMR spectroscopies. The biological screening showed an evident improvement of the activity concerning the antibacterial property in the case of pyrazoline relative to their chalcone precursors. In particular, the pyrazolines distilled in 5a, 5c, and 5f proved to be the most effective in inhibition, especially in *S. aureus*, whereas the chalcones had weak or no inhibitory effects at all, especially on *E. coli*. The results demonstrated that the cyclization reaction leading to the formation of pyrazolines significantly improved bacterial activity, with the presence of electron-giving or removing groups actively influencing efficacy. Subsequent research will include in vitro assays, such as Minimum Inhibitory Concentration and the lowest Bactericidal Concentration, as well as in vivo experiments in suitable animal models to determine pharmacokinetic activities and toxicity.

Acknowledgment: We extend our sincere appreciation to the College of Pharmacy and Dentistry at the University of Sulaimani for their invaluable support.

Author contribution: Zheena Jabar Mustafa: Methodology, Investigation, Data curation, Data collection, Formal analysis, Writing – original draft. **Twana Mohsin Salih**: Conceptualization, Methodology, Supervision, Project administration, Writing – review & editing. **Farouq Emam Hawaiz**: Formal analysis, Validation, Visualization, Writing – review & editing.

Data availability: Data will be available upon reasonable request by the authors.

Conflicts of interest: The authors declare that they have no known competing financial interests or personal relationships that could have appeared to influence the work reported in this paper.

Funding: The authors did not receive support from any organization for the conducting of the study.

References

[1] G. E. Forcados, A. Muhammad, O. O. Oladipo, S. Makama, and C. A. Meseko, "Metabolic implications of oxidative stress and inflammatory process in sars-cov-2 pathogenesis: therapeutic potential of natural antioxidants," *Frontiers in Cellular and Infection Microbiology*., vol. 11, p. 654813, May 2021, doi: 10.3389/fcimb.2021.654813.

[2] K. M. Qadir *et al.*, "Synthesis, molecular docking study and antibacterial activity of new pyrazoline derivatives," *Bulletin of the Chemical Society of Ethiopia,* vol. 39, no. 5, pp. 955-966, 2025, doi: 10.4314/bcse.v39i5.11.

[3] A. Özdemir, G. Turan-Zitouni, Z. Asım Kaplancıklı, G. Revial, F. Demirci, and G. İşcan, "Preparation of some pyrazoline derivatives and evaluation of their antifungal activities," *Journal of Enzyme Inhibition and Medicinal Chemistry*., vol. 25, no. 4, pp. 565–571, Aug. 2010, doi: 10.3109/14756360903373368.

[4] J. O'Neill. "Tackling drug-resistant infections globally: final report and recommendations," London, UK: HM Government & Wellcome Trust, May 2016. Available: https://amr-review.org/sites/default/files/160525_Final%20paper_with%20cover.pdf.

[5] Interagency Coordination Group on Antimicrobial Resistance (IACG). No time to wait: securing the future from drug-resistant infections—report to the Secretary-General of the United Nations. Geneva, Switzerland: World Health Organization, Apr. 2019. Available: https://www.who.int/docs/default-source/documents/no-time-to-wait-securing-the-future-from-drug-resistant-infections-en.pdf.

[6] M. Linden, S. Hofmann, A. Herman, N. Ehler, R. M. Bär, and S. R. Waldvogel. "Electrochemical synthesis of pyrazolines and pyrazoles via [3+2] dipolar cycloaddition," *Angewandte Chemie International Edition*, vol. 62, no. 9, p. e202214820, Feb. 2023, doi:10.1002/anie.202214820.

[7] M. S. Praceka, S. Megantara, R. Maharani, and M. Muchtaridi. "Comparison of various synthesis methods and synthesis parameters of pyrazoline derivatives," *Journal of Advanced Pharmaceutical Technology & Research*, vol. 12, no. 4, pp. 321–326, Oct. 2021, doi: 10.4103/japtr.JAPTR_252_21.

[8] M. R. Shaaban, A. S. Mayhoub, and A. M. Farag. "Recent advances in the therapeutic applications of pyrazolines," *Expert Opinion on Therapeutic Patents*, vol. 22, no. 3, pp. 253–291, Mar. 2012, doi: 10.1517/13543776.2012.667403.

[9] A. Ahmad, A. Husain, S. A. Khan, Mohd. Mujeeb, and A. Bhandari, "Synthesis, antimicrobial and antitubercular activities of some novel pyrazoline derivatives," *Journal of the Saudi Chemical Society*., vol. 20, no. 5, pp. 577–584, Sept. 2016, doi: 10.1016/j.jscs.2014.12.004.

[10] S. K. Ali, A. M. Murwih, K. Melati, K. N. N. S. Nik Mohammad, and M. Musthahimah. "Design, synthesis, characterization, and cytotoxicity activity evaluation of monochalcones and new pyrazoline derivatives," *Journal of Applied Pharmaceutical Science*, vol. 10, no. 8, pp. 20-36, Aug. 2020, doi: 10.7324/JAPS.2020.10803.

[11] B. Evranos Aksöz, S. S. Gürpinar, and M. Eryilmaz, "Antimicrobial activities of some pyrazoline and hydrazone derivatives," *Turkish Journal of Pharmaceutical Sciences*., vol. 17, no. 5, pp. 500–505, Oct. 2020, doi: 10.4274/tjps.galenos.2019.42650.

[12] S. Jang, J.-C. Jung, and S. Oh. "Synthesis of 1,3-diphenyl-2-propen-1-one derivatives and evaluation of their biological activities," *Bioorganic & Medicinal Chemistry*, vol. 15, no. 12, pp. 4098–4105, June 2007, doi: 10.1016/j.bmc.2007.03.077.

[13] M. M. K. Mervat and T. N.-A. Omar. "Synthesis, characterization, anti-inflammatory, and antimicrobial evaluation of new 2-pyrazoline derivatives derived from guaiacol," *Iraqi Journal of Pharmaceutical Sciences*, vol. 32, Suppl., pp. 254–261, Nov. 2023. doi:10.31351/vol32issSuppl.pp254-261.

[14] S. Kumari, S. K. Paliwal, and R. Chauhan. "An improved protocol for the synthesis of chalcones containing pyrazole with potential antimicrobial and antioxidant activity," *Current Bioactive Compounds*, vol. 14, no. 1, pp. 39–47, Apr. 2018, doi:10.2174/1573407212666161101152735.

[15] Y. Vásquez-Martínez *et al.* "Antimicrobial, anti-inflammatory and antioxidant activities of polyoxygenated chalcones," *Journal of the Brazilian Chemical Society*, vol. 30, no. 2, pp. 286–304, 2019, doi:10.21577/0103-5053.20180177.

[16] S. N. A. Bukhari, M. Jasamai, I. Jantan, and W. Ahmad. "Review of methods and various catalysts used for chalcone synthesis," *Mini-Reviews in Organic Chemistry*, vol. 10, no. 1, pp. 73–83, Mar. 2013, doi:10.2174/1570193X11310010006.

[17] S. Mastachi-Loza, T. I. Ramírez-Candelero, L. J. Benítez-Puebla, A. Fuentes-Benítes, C. González-Romero, and M. A. Vázquez. "Chalcones, a privileged scaffold: Highly versatile molecules in [4+2] cycloadditions," *Chemistry – An Asian Journal*, vol. 17, no. 20, p. e202200706, Oct. 2022, doi: 10.1002/asia.202200706.

[18] M. Rani and Y. Mohamad, "Synthesis, studies and in vitro antibacterial activity of some 5-(thiophene-2-yl)-phenyl pyrazoline derivatives," *Journal of Saudi Chemical Society*, vol. 18, no. 5, pp. 411–417, Nov. 2014, doi: 10.1016/j.jscs.2011.09.002.

[19] Y. H. Lee *et al.* "A new synthetic chalcone derivative, 2-hydroxy-3',5,5'-trimethoxychalcone (DK-139), suppresses the Toll-like receptor 4-mediated inflammatory response through inhibition of the Akt/NF-κB pathway in BV2 microglial cells," *Experimental & Molecular Medicine*, vol. 44, no. 6, p. 369, 2012, doi:10.3858/emm.2012.44.6.042.

[20] S. Kumar, S. Bawa, S. Drabu, R. Kumar, and H. Gupta. "Biological activities of pyrazoline derivatives -a recent development," *Recent Patents on Anti-Infective Drug Discovery*, vol. 4, no. 3, pp. 154–163, Nov. 2009, doi: 10.2174/157489109789318569.

[21] M. Mantzanidou, E. Pontiki, and D. Hadjipavlou-Litina. "Pyrazoles and pyrazolines as anti-inflammatory agents," *Molecules*, vol. 26, no. 11, p. 3439, June 2021, doi: 10.3390/molecules26113439.

[22] M. Gomes *et al.* "Chalcone derivatives: promising starting points for drug design," *Molecules*, vol. 22, no. 8, p. 1210, July 2017, doi: 10.3390/molecules22081210.

[23] K. Mezgebe, G. Terfassa, and G. Letebrhan, "Synthesis and pharmacological activities of chalcone derivatives bearing N-heterocyclic moieties," *American Chemical Society Omega*, vol. 8, pp. 35503–35523, 2023, doi: 10.1021/acsomega.3c01035.

[24] S. A. Lahsasni, F. H. Al Korbi, and N. A.-A. Aljaber. "Synthesis, characterization and evaluation of antioxidant activities of some novel chalcones analogues," *Chemistry Central Journal*, vol. 8, no. 1, p. 32, Dec. 2014, doi: 10.1186/1752-153X-8-32.

[25] A. A. WalyEldeen, S. Sabet, H. M. El-Shorbagy, I. A. Abdelhamid, and S. A. Ibrahim. "Chalcones: Promising therapeutic agents targeting key players and signaling pathways regulating the hallmarks of cancer," *Chemico-Biological Interactions*, vol. 369, p. 110297, Jan. 2023, doi: 10.1016/j.cbi.2022.110297.

[26] X. Fang, B. Yang, Z. Cheng, P. Zhang, and M. Yang. "Synthesis and antimicrobial activity of novel chalcone derivatives," *Research on Chemical Intermediates*, vol. 40, no. 4, pp. 1715–1725, Apr. 2014, doi: 10.1007/s11164-013-1076-5.

[27] M. Johnson *et al.*, "Design, synthesis, and biological testing of pyrazoline derivatives of combretastatin-A4," *Bioorganic & Medicinal Chemistry Letters*., vol. 17, no. 21, pp. 5897–5901, Nov. 2007, doi: 10.1016/j.bmcl.2007.07.105.

[28] J. Uddin, S. W. Ali Shah, M. Zahoor, R. Ullah, and A. Alotaibi. "Chalcones: the flavonoid derivatives synthesis, characterization, their antioxidant and in vitro/in vivo antidiabetic potentials," *Heliyon*, vol. 9, no. 11, p. e22546, Nov. 2023, doi: 10.1016/j.heliyon.2023.e22546.

[29] K. V. Sashidhara *et al.* "Identification of quinoline-chalcone hybrids as potential antiulcer agents," *European Journal of Medicinal Chemistry*, vol. 89, pp. 638–653, Jan. 2015, doi: 10.1016/j.ejmech.2014.10.068.

[30] M. H. Nematollahi, M. Mehrabani, Y. Hozhabri, M. Mirtajaddini, and S. Iravani. "Antiviral and antimicrobial applications of chalcones and their derivatives: from nature to greener synthesis," *Heliyon*, vol. 9, no. 10, p. e20428, Oct. 2023, doi: 10.1016/j.heliyon.2023.e20428.

[31] G. B. Souza *et al.* "Synthesis of chalcone derivatives by Claisen-Schmidt condensation and in vitro analyses of their antiprotozoal activities," *Natural Product Research*, vol. 38, no. 8, pp. 1326–1333, Apr. 2024, doi: 10.1080/14786419.2022.2140337.

[32] D. Matiadis and M. Sagnou, "Pyrazoline hybrids as promising anticancer agents: an up-to-date overview," *International Journal of Molecular Sciences*., vol. 21, no. 15, p. 5507, July 2020, doi: 10.3390/ijms21155507.

[33] R. B. Birari, S. Gupta, C. G. Mohan, and K. K. Bhutani, "Antiobesity and lipid lowering effects of Glycyrrhiza chalcones: Experimental and computational studies," *Phytomedicine,* vol. 18, no. 8–9, pp. 795–801, June 2011, doi: 10.1016/j.phymed.2011.01.002.

[34] T. Yamamoto *et al.* "Anti-allergic activity of naringenin chalcone from a tomato skin extract," *Bioscience, Biotechnology, and Biochemistry*, vol. 68, no. 8, pp. 1706–1711, Jan. 2004, doi: 10.1271/bbb.68.1706.

[35] S. Cho *et al.* "Isoliquiritigenin, a chalcone compound, is a positive allosteric modulator of GABAA receptors and shows hypnotic effects," *Biochemical and Biophysical Research Communications*, vol. 413, no. 4, pp. 637–642, Oct. 2011, doi: 10.1016/j.bbrc.2011.09.026.

[36] M. Roucan, M. Kielmann, S. Connon, and M. Senge, "Conformational control of nonplanar free base porphyrins: towards bifunctional catalysts of tunable basicity," *Chemical Communications*, vol. 54, no. 1, pp. 26–29, 2018, doi:10.1039/C7CC08099A.

[37] P. Pinto *et al.* "Chalcone derivatives targeting mitosis: synthesis, evaluation of antitumor activity and lipophilicity," *European Journal of Medicinal Chemistry*, vol. 184, p. 111752, Dec. 2019, doi: 10.1016/j.ejmech.2019.111752.

[38] F. Tok, M. O. Doğan, B. Gürbüz, and B. Koçyiğit-Kaymakçioğlu. "Synthesis of novel pyrazoline derivatives and evaluation of their antimicrobial activity," *Journal of Research in Pharmacy,* vol. 26, no. 5, pp. 1453–1460, 2022, doi: 10.29228/jrp.238.

[39] B.-Y. Shen, Y. Yang, X.-X. Zhao, C. Wu, X.-Y. Zhu, and Y. Li. "Antibacterial efficacy evaluation and mechanism probe of small lysine chalcone peptide mimics," *European Journal of Medicinal Chemistry*, vol. 188, p. 111957, Nov. 2020, doi: 10.1016/j.ejmech.2022.114885.

[40] B. Varghese, S. N. Al-Busafi, F. O. Suliman, and S. M. Z. Al-Kindy. "Unveiling a versatile heterocycle: pyrazoline – a review," *RSC Advances*, vol. 7, no. 74, pp. 46999–47016, 2017, doi: 10.1039/C7RA08939B.

[41] L. Fauzi'ah and T. D. Wahyuningsih. "Synthesis of 1-phenyl-3-(4'-nitrophenyl)-5-(3',4'-dimethoxy-6'-nitrophenyl)-2-pyrazoline and its antibacterial activity". in Proc. 14th Int. Symp. Therapeutic Ultrasound, Las Vegas, NV, USA, 2017, p. 020051, doi: 10.1063/1.4978124.

[42] R. A. Menezes, C. N. Bhuvaneshwari, H. Venkatachalam, and K. S. Bhat. "Focused review on applications of chalcone based compounds in material science," *Discover Applied Sciences*, vol. 7, no. 8, p. 814, Jul. 2025, doi: 10.1007/s42452-025-07478-0.

[43] N. Maciejewska *et al*. "Novel chalcone-derived pyrazoles as potential therapeutic agents for the treatment of non-small cell lung cancer," *Scientific Reports*, vol. 12, no. 1, p. 3703, Mar. 2022, doi: 10.1038/s41598-022-07691-6.

[44] M. Mustafa and Y. A. Mostafa. "A facile synthesis, drug-likeness, and in silico molecular docking of certain new azidosulfonamide–chalcones and their in vitro antimicrobial activity," *Monatshefte für Chemie - Chemical Monthly*, vol. 151, no. 3, pp. 417–427, Mar. 2020, doi: 10.1007/s00706-020-02568-8.

[45] T. Bollenbach, "Antimicrobial interactions: mechanisms and implications for drug discovery and resistance evolution," *Current Opinion in Microbiology*, vol. 27, pp. 1–9, Oct. 2015, doi: 10.1016/j.mib.2015.05.008.

[46] Z. Zhao *et al*., "Pyrazolone structural motif in medicinal chemistry: Retrospect and prospect," E*uropean Journal of Medicinal Chemistry*, vol. 186, p. 111893, Jan. 2020, doi: 10.1016/j.ejmech.2019.111893.

[47] L. L. Silver. "Appropriate targets for antibacterial drugs," *Cold Spring Harbor Perspectives in Medicine*, vol. 6, no. 12, pp. a030239, Dec. 2016, doi: 10.1101/cshperspect.a030239.

[48] S. Mohamady, B. Kralt, S. K. Samwel, and S. D. Taylor. "Efficient one-pot, two-component modular synthesis of 3,5-disubstituted pyrazoles," *ACS Omega*, vol. 3, no. 11, pp. 15566–15574, Nov. 2018, doi: 10.1021/acsomega.8b02304.

[49] A. S. Nair *et al*., "Development of halogenated pyrazolines as selective monoamine oxidase-b inhibitors: deciphering via molecular dynamics approach," *Molecules*, vol. 26, no. 11, p. 3264, May 2021, doi: 10.3390/molecules26113264.

[50] V. F. Traven, D. A. Cheptsov, S. M. Dolotov, and I. V. Ivanov. "Control of the fluorescence of laser dyes by photooxidation of dihydrohetarenes," *Dyes and Pigments*, vol. 158, pp. 104–113, Nov. 2018, doi: 10.1016/j.dyepig.2018.05.023.

[51] F. E. Hawaiz, A. J. Hussein, and M. K. Samad. "One-pot three-component synthesis of some new azo-pyrazoline derivatives," *European Journal of Chemistry*, vol. 5, no. 2, pp. 233–236, Jun. 2014, doi: 10.5155/eurjchem.5.2.233-236.979.

[52] S. Farooq and Z. Ngaini. "Recent synthetic methodologies for chalcone synthesis (2013–2018)," *Current Organic Chemistry and Applied Technologies*, vol. 6, no. 3, pp. 184–192, Sep. 2019, doi: 10.2174/2213337206666190306155140.

[53] V. V. Salian, B. N. Narayana, K. B. Sarojini, and K. Byrappa, "A comprehensive review on recent developments in the field of biological applications of potent pyrazolines derived from chalcone precursors," *Letters in Drug Design & Discovery*, vol. 15, no. 5, pp. 487-503, 2018. doi:10.2174/1570180814666170703164221.

[54] R. S. Sabah, Z. S. Al-Garawi, and M. N. Al-jibouri. "The utilities of pyrazolines encouraged synthesis of a new pyrazoline derivative via ring closure of chalcone, for optimistic neurodegenerative applications," *Mosul Journal of Science*, vol. 33, no. 1, pp. 21–31, Mar. 2022, doi: 10.23851/mjs.v33i1.1067.

[55] N. A. Nordin, A. R. Ibrahim, and Z. Ngaini. "Biological studies of novel aspirin-chalcone derivatives bearing variable substituents," *Journal of Applied Biology*, vol. 11, no. 1, pp. 20–31, Mar. 2020, doi: 10.37231/jab.2020.11.1.185.

[56] K. N. Ganesh, *et al*., "Green chemistry: a framework for a sustainable future," *Environmental Science and Technology Letters*, vol. 8, no. 7, pp. 487–491, Jun. 2021, doi: 10.1021/acs.iecr.1c02213.

[57] T. Taj, R. R. Kamble, T. M. Gireesh, R. K. Hunnur, and S. B. Margankop. "One-pot synthesis of pyrazoline derivatised carbazoles as antitubercular, anticancer agents, their DNA cleavage and antioxidant activities," E*uropean Journal of Medicinal Chemistry*, vol. 46, no. 9, pp. 4366–4373, Sept. 2011, doi: 10.1016/j.ejmech.2011.07.007.

[58] B. Maleki, G. E. Kahoo, and R. Tayebee. "One-pot synthesis of polysubstituted imidazoles catalyzed by an ionic liquid," *Organic Preparations and Procedures International*, vol. 47, no. 6, pp. 461–472, Nov. 2015, doi: 10.1080/00304948.2015.1088757.

[59] B. Maleki, R. Tayebee, M. Kermanian, and S. Sedigh Ashrafi. "One-Pot Synthesis of 1,8-Dioxodecahydroacridines and Polyhydroquinoline using 1,3-Di (bromo or chloro)-5,5-Dimethylhydantoin as a novel and green catalyst under solvent-free conditions," *Journal of the Mexican Chemical Society*, vol. 57, no. 4, Oct. 2017, doi: 10.29356/jmcs.v57i4.192.

[60] Y. Hayashi. "Pot economy and one-pot synthesis," *Chemical Science*, vol. 7, no. 2, pp. 866–880, 2016, doi: 10.1039/C5SC02913A.
[61] I. K. Ugi, B. Ebert, and W. Hörl. "Formation of 1,1'-iminodicarboxylic acid derivatives, 2,6-diketo-piperazine and dibenzodiazocine-2,6-dione by variations of multicomponent reactions," *Chemosphere,* vol. 43, no. 1, pp. 75–81, Apr. 2001, doi: 10.1016/S0045-6535(00)00326-X.
[62] S. Sahu, M. Banerjee, A. Samantray, C. Behera, and M. Azam, "Synthesis, analgesic, anti-inflammatory and antimicrobial activities of some novel pyrazoline derivatives," *Tropical Journal of Pharmaceutical Research*., vol. 7, no. 2, pp. 961–968, June 2008, Available: https://www.tjpr.org/admin/12389900798187/2008_7_2_6.pdf.
[63] R. Filler and R. Saha. "Fluorine in medicinal chemistry: A century of progress and a 60-year retrospective of selected highlights," *Future Medicinal Chemistry*, vol. 1, no. 5, pp. 777–791, Aug. 2009, doi: 10.4155/fmc.09.65.
[64] S. N. A. Bukhari, X. Zhang, I. Jantan, H. Zhu, M. W. Amjad, and V. H. Masand. "Synthesis, molecular modeling, and biological evaluation of novel 1,3-diphenyl-2-propen-1-one based pyrazolines as anti-inflammatory agents," *Chemistry & Biology Drug Design,* vol. 85, no. 6, pp. 729–742, Jun. 2015, doi: 10.1111/cbdd.12457.
[65] C. Zhou and Y. Wang, "Recent researches in triazole compounds as medicinal drugs," *Current Medicinal Chemistry*, vol. 19, no. 2, pp. 239–280, Jan. 2012, doi:10.2174/092986712803414213.
[66] J. Akhtar, A. A. Khan, Z. Ali, R. Haider, and M. Shahar Yar. "Structure-activity relationship (SAR) study and design strategies of nitrogen-containing heterocyclic moieties for their anticancer activities," *European Journal of Medicinal Chemistry*, vol. 125, pp. 143–189, Jan. 2017, doi: 10.1016/j.ejmech.2016.09.023.
[67] B. P. Bandgar *et al.* "Synthesis, biological evaluation, and docking studies of 3-(substituted)-aryl-5-(9-methyl-3-carbazole)-1H-2-pyrazolines as potent anti-inflammatory and antioxidant agents," *Bioorganic & Medicinal Chemistry Letters*, vol. 22, no. 18, pp. 5839–5844, Sept. 2012, doi: 10.1016/j.bmcl.2012.07.080.
[68] K. L. Kees e*t al*. "New potent antihyperglycemic agents in db/db mice: Synthesis and structure−activity relationship studies of (4-substituted benzyl)(trifluoromethyl)pyrazoles and -pyrazolones;" *Journal of Medicinal Chemistry*, vol. 39, no. 20, pp. 3920–3928, Jan. 1996, doi: 10.1021/jm960444z.
[69] S. N. Shelke, G. R. Mhaske, V. D. B. Bonifácio, and M. B. Gawande. "Green synthesis and anti-infective activities of fluorinated pyrazoline derivatives," *Bioorganic & Medicinal Chemistry Letters*, vol. 22, no. 17, pp. 5727–5730, Sept. 2012, doi: 10.1016/j.bmcl.2012.06.072.
[70] D. Matiadis, "Strategies and methods for the synthesis of 2-pyrazolines: recent developments (2012–2022)," *Advanced Synthesis & Catalysis*., vol. 365, no. 12, pp. 1934–1969, June 2023, doi: 10.1002/adsc.202300373.
[71] O. S. Faleye, B. R. Boya, J.-H. Lee, I. Choi, and J. Lee. "Halogenated antimicrobial agents to combat drug-resistant pathogens". *Pharmacological Reviews*, vol. 76, no. 1, pp. 90–141, Jan. 2024, doi: 10.1124/pharmrev.123.000863.
[72] K. Karale, S. J. Takate, S. P. Salve, B. H. Zaware, and S. S. Jadhav. "Synthesis and antibacterial screening of novel fluorine containing heterocycles," *Oriental Journal of Chemistry*, vol. 31, no. 1, pp. 307–315, Mar. 2015, doi: 10.13005/ojc/310135.
[73] Y. Sugiyama, K. Maeda, and K. Toshimoto. "Is ethnic variability in the exposure to rosuvastatin explained only by genetic polymorphisms in OATP1B1 and BCRP or should the contribution of intrinsic ethnic differences in OATP1B1 be considered?," *Journal of Pharmaceutical Sciences*, vol. 106, no. 9, pp. 2227–2230, Sept. 2017, doi: 10.1016/j.xphs.2017.04.074.
[74] D. L. Pavia, A small-scale approach to organic laboratory techniques, 3rd ed., Brooks/Cole Laboratory series for organic chemistry. Belmont, CA: Brooks/Cole, Cengage Learning, 2011. ISBN: 978-1-4390-4932-7.
[75] S. Veerasingam *et al.* "Contributions of Fourier transform infrared spectroscopy in microplastic pollution research: A review," *Critical Reviews in Environmental Science and Technology*, vol. 51, no. 22, pp. 2681–2743, Nov. 2021, doi: 10.1080/10643389.2020.1807450.
[76] F. Hayat, A. Salahuddin, S. Umar, and A. Azam, "Synthesis, characterization, antiamoebic activity and cytotoxicity of novel series of pyrazoline derivatives bearing quinoline tail," *European Journal of Medicinal Chemistry*., vol. 45, no. 10, pp. 4669–4675, Oct. 2010, doi: 10.1016/j.ejmech.2010.07.028.
[77] A. R. Kennedy, Z. R. Kipkorir, C. I. Muhanji, and M. O. Okoth. "4-(Benzyloxy) benzaldehyde," *Acta Crystallographica Section E: Structure Reports Online*, vol. 66, no. 8, pp. o2110–o2110, Aug. 2010, doi: 10.1107/S1600536810027200.
[78] Y. Ma, C. Yang, Z. Li, Z. Li, and J. Ding, "1-(4-Benzyloxy-2-hydroxyphenyl) ethanone," *Acta Crystallographica Section E: Structure Reports Online*, vol. 67, no. 12, pp. o3225–o3225, Dec. 2011, doi:10.1107/S160053681104637X.
[79] S. Sharma, S. Kaur, T. Bansal, and J. Gaba. "Review on synthesis of bioactive pyrazoline derivatives," *Chemical Science Transactions*, vol. 3, no. 3, pp. 861-875, Jun. 2014, doi: 10.7598/cst2014.796.
[80] Y. Baqi and A. H. Ismail. "Microwave-assisted synthesis of near-infrared chalcone dyes: a systematic approach," *ACS Omega*, vol. 10, no. 7, pp. 7317–7326, Feb. 2025, doi: 10.1021/acsomega.4c11066.
[81] B. Salehi, *et al.,* "Pharmacological properties of chalcones: A review of preclinical including molecular mechanisms and clinical evidence," Frontiers in Pharmacology, vol. 11, p. 592654, Jan. 2021. doi:10.3389/fphar.2020.592654.M.
[82] S. Gok, M. Murat Demet, A. Özdemir, and G. Turan-Zitouni, "Evaluation of antidepressant-like effect of 2-pyrazoline derivatives," *Medicinal Chemistry Research*., vol. 19, no. 1, pp. 94–101, Feb. 2010, doi: 10.1007/s00044-009-9176-x.
[83] R. H. H. Salih *et al.* "One-pot synthesis, molecular docking, ADMET, and DFT studies of novel pyrazolines as promising SARS-CoV-2 main protease inhibitors," *Research on Chemical Intermediates,* vol. 48, no. 11, pp. 4729–4751, Nov. 2022, doi: 10.1007/s11164-022-04831-5.
[84] T. Taj, R. R. Kamble, T. M. Gireesh, R. K. Hunnur, and S. B. Margankop, "One-pot synthesis of pyrazoline derivatised carbazoles as antitubercular, anticancer agents, their DNA cleavage and antioxidant activities," *European Journal of Medicinal Chemistry*., vol. 46, no. 9, pp. 4366–4373, Sept. 2011, doi: 10.1016/j.ejmech.2011.07.007.
[85] S. O. Mamand, D. Abdul, and F. E. Hawaiz. "Traditional, one-pot three component synthesis and anti-bacterial evaluations of some new pyrazoline derivatives," *Egyptian Journal of Chemistry,* vol. 65, no. 10, pp. 239-248, Oct. 2022, doi: 10.21608/ejchem.2022.129819.5727.

[86] J. Hudzicki, "Kirby-Bauer disk diffusion susceptibility test protocol," *American Society for Microbiology*, Dec. 2009. Available: https://asm.org/getattachment/2594ce26-bd44-47f6-8287-0657aa9185ad/kirby-bauer-disk-diffusion-susceptibility-test-protocol-pdf.pdf.

[87] D. Olender *et al*. "Bis-chalcones obtained via one-pot synthesis as the anti-neurodegenerative agents and their effect on the HT-22 cell line," *Heliyon*, vol. 10, no. 17, p. e37147, Sept. 2024, doi: 10.1016/j.heliyon.2024.e37147.

[88] C. J. Thomson, D. M. Barber, and D. J. Dixon. "One-pot catalytic enantioselective synthesis of 2-pyrazolines," *Angewandte Chemie International Edition*, vol. 58, no. 8, pp. 2469-2473, 2019, doi: 10.1002/anie.201811471.

[89] T. A. Fitri, R. Hendra, and A. Zamri. "One-pot synthesis and molecular docking study of pyrazoline derivatives as an anticancer agent: Pyrazoline derivatives as an anticancer agent," *Pharmacy Education*, vol. 23, no. 2, pp. 260–265, June 2023, doi: 10.46542/pe.2023.232.260265.

[90] S. Farooq and Z. Ngaini. "One-pot and two-pot synthesis of chalcone based mono and bis-pyrazolines," *Tetrahedron Letters*, vol. 61, no. 4, p. 151416, Jan. 2020, doi: 10.1016/j.tetlet.2019.151416.

[91] C. Shekhar Yadav *et al*., "Recent advances in the synthesis of pyrazoline derivatives from chalcones as potent pharmacological agents: A comprehensive review," *Results in Chemistry*., vol. 7, p. 101326, Jan. 2024, doi: 10.1016/j.rechem.2024.101326.

[92] V. Lellek, C. Chen, W. Yang, J. Liu, X. Ji, and R. Faessler. "An efficient synthesis of substituted pyrazoles from one-pot reaction of ketones, aldehydes, and hydrazine monohydrochloride," *Synlett*, vol. 29, no. 08, pp. 1071–1075, May 2018, doi: 10.1055/s-0036-1591941.

[93] M. R. Shaaban, A. S. Mayhoub, and A. M. Farag, "Recent advances in the therapeutic applications of pyrazolines," *Expert Opinion on Therapeutic Patents*, vol. 22, no. 3, pp. 253–291, Mar. 2012, doi: 10.1517/13543776.2012.667403.

[94] D. C. Kaseman *et al.*, "Chemical analysis of fluorobenzenes via multinuclear detection in the strong heteronuclear j-coupling regime," *Applied Sciences*, vol. 10, no. 11, p. 3836, 2020. doi: 10.3390/app10113836.

[95] A. Ahmad, A. Husain, S. A. Khan, M. Mujeeb, and A. Bhandari, "Synthesis, antimicrobial and antitubercular activities of some novel pyrazoline derivatives," *Journal of Saudi Chemical Society*, vol. 20, no. 5, pp. 577-584, Sep. 2016, doi: 10.1016/j.jscs.2014.12.004.

[96] S. Gomha, M. Abdallah, M. Abd El-Aziz, and N. Serag. "Ecofriendly one-pot synthesis and antiviral evaluation of novel pyrazolyl pyrazolines of medicinal interest," *Turkish Journal of Chemistry*, vol. 40, pp. 484–498, 2016, doi: 10.3906/kim-1510-25.

[97] M. A. Romero Reyes, S. Dutta, M. Odagi, C. Min, and D. Seidel. "Catalytic enantioselective synthesis of 2-pyrazolines via one-pot condensation/6π-electrocyclization: 3,5-bis(pentafluorosulfanyl)-phenylthioureas as powerful hydrogen bond donors," *Chemical Science*., vol. 15, no. 37, pp. 15456–15462, 2024, doi: 10.1039/D4SC04760E.

[98] S. Mishra *et al*. "Ferrocenyl–cymantrenyl hetero-bimetallic chalcones: synthesis, structure and biological properties," *Journal of Molecular Structure*, vol. 1085, pp. 162–172, Apr. 2015, doi: 10.1016/j.molstruc.2014.12.070.

[99] I. Saleh *et al*. "Design, synthesis, and antibacterial activity of N -(trifluoromethyl)phenyl substituted pyrazole derivatives," *RSC Medicinal Chemistry*, vol. 12, no. 10, pp. 1690–1697, 2021, doi: 10.1039/D1MD00230A.

[100] M. M. Kandeel, N. A. Abdou, H. H. Kadry, and R. M. El-Masry. "Synthesis and antitumor activity of some novel heterocyclic compounds derived from chalcone analogues," *Organic Chemistry*, 2014. Available: https://repository.msa.edu.eg/items/1212f5a9-3889-43b5-ad5b-1d6514a67b54/full.

[101] C. Zhuang, W. Zhang, C. Sheng, W. Zhang, C. Xing, and Z. Miao. "Chalcone: a privileged structure in medicinal chemistry," *Chemical Reviews*, vol. 117, no. 12, pp. 7762–7810, June 2017, doi: 10.1021/acs.chemrev.7b00020.

[102] N. Das, B. Dash, M. Dhanawat, and S. Shrivastava, "Design, synthesis, preliminary pharmacological evaluation, and docking studies of pyrazoline derivatives," *Chemical Papers*., vol. 66, no. 1, pp. 67-74, Jan. 2012, doi: 10.2478/s11696-011-0106-2.

[103] Md. A. Rahman and A. A. Siddiqui. "Pyrazoline derivatives: a worthy insight into the recent advances and potential pharmacological activities," *International Journal of Pharmaceutical Sciences and Drug Research*, vol. 2, no. 3, pp. 165–175, July 2010, doi: 10.25004/IJPSDR.2010.020302

[104] Z. A. Kaplancıklı, A. Özdemir, G. Turan-Zitouni, M. D. Altıntop, and Ö. D. Can. "New pyrazoline derivatives and their antidepressant activity," *European Journal of Medicinal Chemistry*, vol. 45, no. 9, pp. 4383–4387, Sept. 2010, doi:' 10.1016/j.ejmech.2010.06.011.

[105] M. Al-Anazi, M. N. El-Nabi, A. El-Ashmawy, and A. A. Al-Majid, "Synthesis, anticancer activity and docking studies of pyrazoline and pyrimidine derivatives as potential epidermal-growth-factor-receptor (EGFR) inhibitors," *Arabian Journal of Chemistry*, vol. 14, no. 10, pp. 103397, Oct. 2021. doi: 10.1016/j.arabjc.2022.103864.

[106] S. Hassan. "Synthesis, antibacterial and antifungal activity of some new pyrazoline and pyrazole derivatives," *Molecules*, vol. 18, no. 3, pp. 2683–2711, Feb. 2013, doi: 10.3390/molecules18032683.

[107] D. Havrylyuk, O. Roman, and R. Lesyk, "Synthetic approaches, structure activity relationship and biological applications for pharmacologically attractive pyrazole/pyrazoline–thiazolidine-based hybrids," *European Journal of Medicinal Chemistry*., vol. 113, pp. 145–166, May 2016, doi: 10.1016/j.ejmech.2016.02.030.